## Title
Section-Related Measures of Traffic System Performance: Prototype Field Implementation



## Authors
Ritchie, Stephen G.
Sun, Carlos
Oh, Seri
et al.

## Publication Date
2001-10-01

CALIFORNIA PATH PROGRAM
INSTITUTE OF TRANSPORTATION STUDIES
UNIVERSITY OF CALIFORNIA, BERKELEY

# Section-Related Measures of Traffic System Performance: Prototype Field Implementation

**Stephen G. Ritchie, Carlos Sun, Seri Oh, Cheol Oh**
*University of California, Irvine*

**California PATH Research Report**
**UCB-ITS-PRR-2001-32**

This work was performed as part of the California PATH Program of the University of California, in cooperation with the State of California Business, Transportation, and Housing Agency, Department of Transportation; and the United States Department of Transportation, Federal Highway Administration.



Final Report for MOU 336

October 2001

ISSN 1055-1425

**California PATH**

**(Partners for Advanced Transit and Highways)**

**MOU 336 Final Report**

# Section-Related Measures of Traffic System Performance: Prototype Field Implementation

**Stephen G. Ritchie**

**Carlos Sun***

**Seri Oh**

**Cheol Oh**

**Institute of Transportation Studies**

**University of California**

**Irvine, CA 92697-3600**

**July, 2001**

* Formerly Department of Civil and Environmental Engineering, Rowan University, Glassboro, NJ 08028; currently, Department of Civil and Environmental Engineering, University of Missouri, Columbia, MO 65211

**ACKNOWLEDGEMENT**

This work was performed as part of the California PATH Program of the University of California, in cooperation with the State of California Business, Transportation and Housing Agency, Department of Transportation; and the United States Department of Transportation, Federal Highway Administration.

The contents of this report reflect the views of the authors who are responsible for the facts and the accuracy of the data presented herein. The contents do not necessarily reflect the official views or policies of the State of California. This report does not constitute a standard, specification, or regulation.

The authors gratefully acknowledge the assistance of Richard Nelson, City of Irvine, Joe Palen, California Department of Transportation; and Steve Hilliard, Inductive Signature Technologies, Inc., in conducting this research.

**ABSTRACT**

In this project (MOU 336), an initial phase of a field implementation was accomplished of the results of a previous research project (MOU 224), in which a vehicle reidentification algorithm based on loop signature analysis was developed using freeway traffic data. This algorithm was extended to non-freeway cases, initially using a section of 2-lane major arterial in cooperation with the City of Irvine, California. The technique was enhanced to address problems such as "irregularities" in vehicle signatures associated with trucks, tail-gating vehicles and erroneous counting of vehicles, with the objective of obtaining 100% correct counts at each station. The enhanced algorithm was also applied to a major specially instrumented signalized intersection in Irvine, California to demonstrate acquisition of data for real-time congestion monitoring, incident detection and level of service measurement. The initial application was for through vehicles on one approach. In order to achieve more reliable vehicle reidentification results, additional routines for vehicle movement filtering at the downstream station were applied. Reidentification results based on an initial dataset showed an encouraging matching result of 84.07% overall, for individual vehicles. Speed estimation from a single loop signature was one of the applications investigated in detail. For several study sites, the vehicle reidentification matching rates, using speed estimated from a single loop, were only slightly lower than for double loops. In another detailed application (using freeway data collected in previous PATH project MOU 224), vehicle classification using a Backpropagation Neural Network showed an 80 % classification rate overall for all vehicle types. Heuristic approaches to vehicle classification also demonstrated good results.

**Keywords**

vehicle signature, inductive loop detector, single loop speed estimation, vehicle classification, vehicle reidentification

**EXECUTIVE SUMMARY**

With the existing widespread use of inductive loop detectors (ILDs), Intelligent Transportation Systems (ITS) have a constant source of information on traffic system conditions. However, ILDs typically provide only point measures of traffic characteristics such as volume, occupancy, and depending on the loop configuration, local speed, which are inadequate for many ITS applications. If these detectors could be used in a "smarter" way, more useful information could be obtained for important ITS applications in traveler information and route guidance systems, congestion monitoring and incident detection, and traffic control via freeway ramp meters, surface street signals and changeable message signs. One technique to obtain significantly more information from ILDs is to utilize the vehicle waveforms that are produced when each vehicle passes over a loop. Such waveforms are essentially "signatures" that can be reidentified at downstream stations, and yield more useful information such as real-time section travel times, section speed, and section density, as well as vehicle classification and origin-destination data.

In this project (MOU 336), an initial phase of a field implementation was accomplished of the results of a previous research project (MOU 224), in which a vehicle reidentification algorithm based on loop signature analysis was developed using freeway traffic data. This algorithm was extended to non-freeway cases, initially using a section of 2-lane major arterial in cooperation with the City of Irvine, California. The technique was enhanced to address problems such as "irregularities" in vehicle signatures associated with trucks, tail-gating vehicles and erroneous counting of vehicles, with the objective of obtaining 100% correct counts at each station.

The enhanced algorithm was also applied to a major specially instrumented signalized intersection in Irvine, California to demonstrate acquisition of data for real-time congestion monitoring, incident detection and level of service measurement. The initial application was for through vehicles on one approach. In order to achieve more reliable vehicle reidentification results, additional routines for vehicle movement filtering at the downstream station were applied. Reidentification results based on an initial dataset showed an encouraging matching result of 84.07% overall, for individual vehicles. On-line real-time vehicle reidentification operation (for the same approach, but for all three departure movements: left, though and right), and a Graphical User Interface for the algorithm are being developed under another PATH project (MOU 3008).

Speed estimation from a single loop signature was one of the applications investigated in detail. For several study sites, the vehicle reidentification matching rates, using speed estimated from a single loop, were only slightly lower than for double loops. In another detailed application (using freeway data collected in a previous PATH project, MOU 224), vehicle classification using a Backpropagation Neural

Network showed an 80 % classification rate overall for all vehicle types. Heuristic approaches to vehicle classification also demonstrated good results.

This study has significantly advanced a new framework based on conventional inductive loop detectors that has now been shown capable of estimating freeway, arterial and intersection measures of traffic performance, including section speed and travel time, section density, and vehicle travel time through a signalized intersection, among others. It has been shown that quite accurate estimates of vehicle speed can be obtained from single inductive loop detectors instead of the double loops previously used in this research, greatly expanding the potential for application of loop-based vehicle reidentification techniques. The potential was also demonstrated for real-time derivation of vehicle classification information from inductive signatures.

In summary, this research has shown that low-cost enhancements to the preexisting traffic surveillance infrastructure can be an economically attractive means of obtaining expanded and more accurate traffic performance and travel information. Applications of such vehicle reidentification concepts show encouraging results for potential direct use in providing network-wide travel information.

**TABLE OF CONTENTS**

## 3. LIST OF FIGURES

**LIST OF TABLES**

**List of Figures**

**List of Tables**

# MOU 336 Section-Related Measures of Traffic System Performance: Prototype Field Implementation

## CHAPTER 1 INTRODUCTION

### 1.1 Background

As new exciting technologies are being developed for transportation applications and new Intelligent Transportation Systems (ITS) are being tested and implemented, there is a growing need for more detailed and accurate transportation data. Researchers are currently exploring the use of various new forms of detectors and surveillance systems, including technologies such as infrared, microwave, ultrasonic, acoustic, Automatic Vehicle Identification (AVI), piezo-electric, magnetic, Global Positioning System (GPS), cellular modem, and video image processing. In addition to investigating new technologies, there is the opportunity to squeeze out more information from the current detector infrastructure, which mostly consists of inductive loop detectors (ILDs). One technique to obtain significantly more information from ILDs is to utilize the vehicle waveforms that are produced when a vehicle passes over a loop. Previously, inductive loop detector cards only operated in a pulse or a presence mode, producing a digital output. However, detector manufacturers are now producing detectors that have the capability to output a vehicle waveform through a serial port on the detector card. This waveform is essentially an inductive signature that is the result of the net decrease in inductance when a vehicle's metallic mass passes over the magnetic field generated by the inductive loop. By analyzing vehicle signatures, transportation data that are difficult to acquire, such as link or section travel times or speeds, traffic densities, and lane changes, as well as single loop speeds, dynamic origin/destination demands, and vehicle classification, can be obtained.

In this project (PATH MOU 336), a real-time prototype field implementation was accomplished of the results of a previous PATH research project (PATH MOU 224), in which an off-line vehicle reidentification algorithm based on loop signature analysis was developed using freeway traffic data. This algorithm was modified and extended for the non-freeway case, initially using a section of 2-lane major arterial in cooperation with the City of Irvine, California. The technique was also enhanced to address problems such as "irregularities" in vehicle signatures, with the objective of obtaining 100% correct counts at each station. The enhanced algorithm was also applied to a major instrumented signalized intersection in the City of Irvine to acquire data for applications such as real-time congestion monitoring, incident detection and level of service measurement. In addition, several applications of loop signature analysis were investigated in detail, including the estimation of vehicle speeds from single ILDs, and the categorization of vehicles into predefined classes based on their signatures ("vehicle classification").

## 1.2 Report Outline

The following chapter describes the two study sites, the loop signature data collection setup, and some example vehicle signatures. Chapters 3 and 4 focus on the vehicle signature applications of single loop speed estimation, and vehicle classification, respectively. Chapter 5 describes the vehicle reidentification algorithm and its enhancement. Chapter 6 presents the initial results obtained from applying the enhanced algorithm, and Chapter 7 summarizes the the conclusions of this research.

# CHAPTER 2 STUDY SITES AND DATA COLLECTION

## 2.1 Study Site Description

To enhance, test and evaluate the vehicle reidentification algorithm, two new study sites in the City of Irvine, California were selected in close cooperation with City staff. This chapter contains descriptions of the study sites, hardware and software implementation, as well as the data collection setup. Chapter 4 discusses the analysis of vehicle reidentification data from a previous data collection effort (in PATH MOU 224) for purposes of developing a vehicle classification capability. That data set and site are described in Chapter 4.3.2.

### 2.1.1 Alton Parkway

This site consisted of two detector stations bounding a two-lane section of Alton Parkway between the intersections of Telemetry and Jenner in Irvine, California. The distance between the two loop stations was 425 feet. Figure 1 shows this study site and video camera setup for ground truthing purposes. The downstream detector station at this site was located right before the left turn bay. Due to this configuration some "irregular" signatures were generated at this site, and these are discussed further in Chapter 5.

### 2.1.2 Intersection of Alton Parkway and Irvine Center Drive

The second study site is the intersection of Alton Parkway and Irvine center Drive (Alton/ICD), an eight phase fully actuated intersection in the City of Irvine, California. All approaches were divided with a raised median, had exclusive double left turn lanes, and an exclusive right turn lane. There were three lanes for through movements on each approach. Each approach also had a set of double loops, referred to as approach loops. These loops were at 325 ~ 375 feet from the intersection, except for the eastbound Alton loops which were about 800 feet upstream of the intersection. Additionally, there were sets of double loops in each lane right after the intersection, referred to as departure loops. This brought the total number of loops at the intersection to 48. Some of these loops were specially installed for this research project. The intersection of Alton/ICD is the only intersection in the City equipped with double loops on all four approaches and departures, making it uniquely suitable for this project. The nearest intersection from each approach is about 100 ~ 200 feet upstream from the approach loops. The Alton/ICD intersection is shown in Figure 2.

## 2.2 Data Collection Equipment and Setup

### 2.2.1 Alton Parkway

The loops at this site were standard 1.83mX1.83m (6ftX6ft) rectangular loops that are commonly used by many state and city agencies. Video surveillance was instrumented as needed on each lane at both the upstream and downstream stations. Video was used for ground truthing of vehicles, to confirm the flow values obtained from the detectors, and to check the road traffic conditions. Data were collected using 3M detector cards in the controller box. Using the data collection software "Siglog", developed by subcontractor Gardner System, the vehicle signatures were saved in a laptop. The signature data collection interval varied according to the sensitivity level of the detector card. In our case, sensitivity level 3 was set as a default to obtain sufficiently detailed signatures. Sensitivity level 3 corresponds to about a 7 ms scan rate. For example, whenever a vehicle passed over the loop, the inductance change was recorded about every 7ms and used to produce vehicle signatures. Figure 3 illustrates the data collection and transmission setup.

There were two data collection periods. The morning peak data were collected between approximately 8:00am and 9:30am. This dataset contained 581 vehicle signature pairs. The average flow over that time period was 612 VPH for two lanes. The midday data were collected between approximately 12:00pm and 1:00pm at the upstream station. This dataset contained 530 vehicle signature pairs. The average flow over the midday period was 575 VPH.

### 2.2.2 Alton/ICD Intersection

At this site, the City of Irvine provided and installed a "P" cabinet on the corner of the intersection next to the traffic signal cabinet. The cabinet consisted of four detector racks, each with its own 24v dc power supply. Each rack could hold eight 3M model 822 loop detector cards (24 such dual loop detector cards are needed to fully instrument the intersection). The cabinet contained one Eagle model 2070 controller. At the conclusion of the project, two 2070 controllers (both from a previous PATH project) were installed. The second controller was used for PATH MOU 3008. The 2070 controller software was a special program called "dcol" (data collection) written by Gardner Systems to receive serial data from the detector cards, compare the inductance value against a user set threshold and create a record of the inductive signature for that event. The signature was then time-stamped and sent out the serial port. A PC program called "siglog" (signature log) was also written by Gardner Systems to receive the record sent by the controller. It read the header information to see what loop it came from and placed the record in the appropriate file for storage. The siglog program could be stopped and restarted at any time creating a new set of files so the previous files could be downloaded onto a Zip drive.

Implementation of data collection and analysis at this site was proposed in stages. This project (MOU 336) represented Stage 1 of the implementation, to test both the hardware and software in a limited configuration and to shake out any problems. The Eastbound through lanes on Alton Parkway were used for this purpose.

An associated and ongoing PATH project (MOU 3008) was to be Stage 2. In this stage, the Eastbound Alton approach was still to be used but all of the three exits or departures were to be monitored. This configuration allows more complete testing of the reidentification algorithms.

In the future, Stage 3 could utilize all approaches at the intersection so that all movements are simultaneously addressed.

As indicated above, in stage one, only eastbound Alton through movements were considered. After two field data collection tests in February, 2000, it was determined that the 2070 controller could only handle one lane in order to obtain sufficiently detailed vehicle signatures. The lane that is nearest to the median was selected as our data collection lane. Three video cameras recorded vehicle movements for ground truthing. The first camera was located at the upstream loop station, 800 feet away from the intersection. A second camera, which was at the intersection stopline, captured all the turning vehicles that were coming from the same upstream loop station. A third camera was used to record downstream traffic flow. The collected data set was composed of light traffic (182 VPHPL) and contained approximately 152 vehicles. The time to collect the data was from 11:45 am to 12:35 pm. There was no network connection from the field to the Irvine TMC and only one 2070 controller was used. Collected data were stored in a laptop using the Siglog software. The above process is illustrated in Figure 4

In MOU 3008 (stage two), the data collection range was extended to one intersection approach and all its three exits. This setup captured all the vehicles from the upstream station for any downstream traffic movement (U-turns were not considered). Eastbound Alton was again selected as the upstream station in this stage. Two 2070 controllers, one for Alton detectors and the other for ICD detectors, were used. Extensive tests were conducted using double loops at each station and 12 detector cards in one 2070 controller. However, to maintain this design, the scan rate of the detectors had to be slowed down, causing significant vehicle signature problems. This limitation required two lanes to be modified from a double loop configuration to a single loop configuration. This enabled the 2070 controllers to scan the detectors at the maximum rate without missing any data.

Loop signature data were sent in real-time to a remote PC at the Irvine Transportation Center (ITC) through two dedicated modems. The siglog software was installed on the ITC PC to save transmitted data in text file format for the reidentification algorithm. This setup is illustrated in Figure 5. The research associated with this configuration is not described further in this report, and can be found in the final report for MOU 3008.

Stage three proposed data collection for the entire intersection, and real-time network connections from the field to the Irvine TMC and UCI labs. The ITC PC and the Irvine TMC would be connected through a City of Irvine Local Area Network (LAN). Also, a real-time connection to UCI Testbed facilities using City Wide Area Network (WAN) would be investigated. Four City of Irvine intersection cameras might be available for video ground truth data collection. A link between the intersection cameras and the UCI Testbed facilities would also be considered. Figure 6 illustrates the proposed network connections.

### 2.3 Example signatures

A vehicle signature actually represents a change in inductance in the electric current of the loop detector due to the iron present in a vehicle. Therefore, different (but repeatable) signatures are generated for different vehicle types and this represents the core idea of the vehicle reidentification concept. Figures 7-11 show some example signatures for different vehicle types. The horizontal axis in each case is proportional to time. Two waveforms were generated for each vehicle because double loop detectors were used. The maximum magnitude of the signatures varies between vehicles because of differences in vehicle types and vehicle clearances above the loops.

# CHAPTER 3 SINGLE LOOP SPEED ESTIMATION

## 3.1 Introduction

Speed is a fundamental traffic variable that is applicable to both macroscopic and microscopic analysis. Individual vehicle speed is the distance traveled divided by the time taken to traverse that distance. In other words, speed measures the rate of motion. The inverse of speed is travel time which is a very useful performance indicator of the transportation supply system. However, speeds are usually measured at points (over short distances) while travel times are used to indicate the duration of travel over a section of roadway or an entire trip. It is therefore necessary to sample speed at multiple points on a section in order to obtain an accurate estimate of the travel time. If an extensive inductive loop infrastructure exists, then travel times can be estimated accurately even during congested traffic conditions. The collection of accurate vehicle speeds for deriving travel times is therefore critical to government agencies, travellers, and university researchers for applications ranging from real-time traffic control to long term transportation planning.

## 3.2 Review

There is significant ongoing research in the area of traffic surveillance. Old technologies are constantly being refined while new technologies are being developed for use in transportation. Evaluation of different detection technology have been performed at different levels of government. For example, Hughes and JHK & Associates (1994) investigated detection technologies for the United States Department of Transportation and the Federal Highway Administration. On the state level, for example, Bahler et al. (1998) tested non-intrusive traffic detection technologies for the Minnesota Department of Transportation. A useful reference on traffic detector technologies is the Traffic Detector Handbook published by the Institute of Transportation Engineers (ITE, 1990). Some technologies that are capable of measuring speed either directly or via post-processing include: inductive loop, piezoelectric, radar, acoustic, ultrasonic, video, and magnetic (Klein, 1995). Even though many new technologies have great potential for future widespread implementation, it is also valuable to improve current detection technology. This is specially relevant to inductive loop detectors, since there is a significant existing infrastructure. For example, in the state of California alone, the California Department of Transportation estimates that there are approximately 300,000 existing inductive loop detectors on California freeways (PATH 1997). This number does not include the significant number of loops deployed in individual cities.

There are two ways of measuring speed using inductive loop detectors. The first way is to use a set of double loops in a speed trap configuration. The speed trap refers to the measurement of the time that a vehicle requires to travel between two detection points (Woods et al., 1994). Woods et al. also discuss other aspects of the speed trap design including optimum speed trap spacing. Speed is measured as

$$v = \frac{d}{t_{on}^{2} - t_{on}^{1}}$$

Where:

$v$ = speed

$d$ = distance between detectors

$t_{on}^{1}$ = time when the first detector turns on

$t_{on}^{2}$ = time when the second detector turns on

In addition to the turn on times, the Traffic Control Systems Handbook (Wilshire et al., 1985) recommends the use of turn off times also in order to improve the speed accuracy. The averaging of the turn on and off times results in the following equation:

$$v = \frac{1}{2}\left(\frac{d}{t_{on}^{2} - t_{on}^{1}} + \frac{d}{t_{off}^{2} - t_{off}^{1}}\right)$$

Where:

$t_{off}^{1}$ = time when the first detector turns off

$t_{off}^{2}$ = time when the second detector turns off

The second way of measuring speed is by using a single loop detector. In other words,

$$v = \frac{l}{t_{off} - t_{on}}$$

Where:

$l$ = effective length, vehicle length + detector length

$t_{on}$ = time when the detector turns on

$t_{off}$ = time when the detector turns off

Since actual vehicle lengths are not known, a mean vehicle length must be assumed for this computation. Because lengths can vary greatly from vehicle to vehicle, the use of a mean vehicle length can result in inaccurate

measurements of speed. For example, longer trucks will produce underestimated speeds, and shorter passenger cars will produce overestimated speed.

Another approach of estimating average speed using single loops is by using fundamental traffic flow considerations. The average speed is estimated by using average lane volume and loop occupancy. Some publications that discuss this approach include Athol (1965), Hall et al. (1989), and Jacobson et al. (1989). Speed is expressed in these approaches as

$$v = \frac{q}{o * g}$$

Where:

$v$ = space mean speed

$q$ = flow

$o$ = occupancy

$g$ = factor that takes into account the vehicle and detector length

Hall et al. discusses the use of a sliding value of g which changes with occupancy and is calibrated separately for each set of geometric conditions. This approach assumes that traffic flow is uniform, occupancy is a constant multiple of density, and vehicle lengths are constant. Speed inaccuracies result when the assumed conditions are invalid. Mikhalkin et al. (1972) shows that an estimate using this approach will produce a biased estimate of the space mean speed. Also, individual vehicle speeds are not estimated with this approach.

In order to produce an unbiased estimate of individual and mean speed using single loops, Mikhalkin et al. (1972) suggests the use of the minimum mean square error estimator for speed. This approach assumes that random vehicle arrival times are uniformly distributed. This approach also necessitates the estimation of the unbiased mean vehicle length during the relevant time interval.

The use of single loop vehicle waveforms for measuring speed has many advantages over previous approaches of speed derivation using loops. First, it can be implemented with existing single loop infrastructure without cutting new loops for speed traps. Second, there is no assumption of a mean vehicle length, so the accuracy of computing speed is not a function of the distribution of vehicle lengths. Third, in contrast to "traffic flow approaches", there is no assumption of traffic uniformity, and individual vehicle speeds in addition to mean speeds can be obtained. Last, there is no distributional assumptions made on vehicle arrival times or vehicle speeds.

### 3.3 Methodology

As was shown from Figure 7 to Figure 11, the vehicle inductive waveforms contain both a leading and a trailing edge. These edges are slew rates which represent the rate of the metallic mass of the vehicle moving over the loop magnetic field. The waveform within these edges is produced when the entire vehicle is covering the loop. This portion of the waveform is no longer the slew rate because of the integration property of the loops, and produces no useful speed information. The estimation of vehicle speed using single inductive loop detectors involves two main procedures. The first is the extraction of the vehicle slew rate or edges from the inductive vehicle waveform. The second is the estimation of the vehicle speed based on the slew rate.

#### 3.3.1 Slew Rate Extraction

There are several steps to extracting the slew rate information from the inductive vehicle waveform. Figure 12a. shows one example of a vehicle waveform that will be used to illustrate the process of slew rate extraction. The y-axis has units of percentage change of inductance counts, and the x-axis has units of milliseconds. Note that the vehicle waveform which results from decreases in inductance have been inverted to facilitate analysis. The first step in extracting slew rates is to eliminate waveform oscillations that have inductance values near the baseline inductance. This is accomplished by using a arbitrary threshold that will eliminate all oscillations while preserving as much waveform information as possible. A value of 10%-20% was found to be a good threshold from empirical trials with different datasets. The oscillations near the baseline occur because the detector card is constantly trying to adjust the base inductance value in order to compensate for changes in absolute inductance due to environmental and other effects. The oscillations also occur because vehicles are composed of a complex combination of metallic masses including the undercarriage, the engine, and axles. Figure 12b shows an example of a waveform with the oscillations removed.

The next step is to extract the leading and trailing edges of the vehicle waveform. These edges are slew rates in the sense that they represent the rate of movement of the vehicle's metallic mass over time. The waveform edges in this case have units of % inductance change over time. The upper end of the waveform edges are found by detecting a local maximum point in the vehicle waveform. Therefore the termination point of the waveform edge is defined as

$$f(x) \leq f(c), \forall x \in S$$

Where:

$c$ = the time at which the local maximum occurs

$f(c)$ = the local maximum

$f(x)$ = the value of the waveform or inductance change at a time x

$S$ = the set of time values that include a single local maximum

Since the waveform is actually a discrete waveform, the termination point of the leading and trailing edges are found by searching for a local maximum by starting from the threshold value that is illustrated in Figure 3b. The resulting leading and trailing edges are shown as solid curves in Figure 12c.

### 3.3.2 Data Description

Data were collected from Alton Parkway, one of our study sites. As mentioned before, there were two data collection periods. The morning peak data was collected between approximately 8:00am and 9:30am at the downstream station. This dataset contained 581 vehicle signature pairs. The average flow over that time period was 612 VPH for two lanes. Due to arterial signalization and varying traffic demand, different speeds, acceleration profiles, and traffic flow levels were observed during the 1-1/2 hour period. The maximum observed speed was 30.66m/s (68.68mph). The minimum speed was 5.47m/s (12.25mph). The arithmetic mean speed was 20.77m/s (46.52mph). The standard deviation of the speed was 4.11m/s. The longest electronic length (length of detector+vehicle) observed was 20.31m. The shortest electronic length observed was 3.89m. The mean electronic length was 4.83m.

The midday data was collected between approximately 12:00pm and 1:00pm at the upstream station. This dataset contained 530 vehicle signature pairs. The average flow over the midday period was 575 VPH. The maximum observed speed was 32.52m/s. The minimum speed was 15.16m/s. The arithmetic mean speed was 22.13m/s. The standard deviation of the speed was 2.61m/s.

Figure 13 shows the percent relative frequency speed distributions for the two datasets. Both the morning and midday datasets contained a wide range of traffic flow conditions and vehicle speeds. This diversity is useful for developing and testing speed computation algorithms. The two datasets were collected from two different sites at different times of the day. Therefore these datasets can be used to test the transferability of the algorithms. Both

datasets also contained a wide range of vehicle types including minivans, sports utility vehicles, trucks, buses, and semi-trailer trucks.

### 3.3.3 Speed Estimation

The first step in the development of the speed computation algorithms is to plot the available data and to analyze the data graphically. Figure 14 confirms our intuition that the slew rate is linearly correlated with speed. The correlation coefficient for the slew rate and speed is 0.8866 for morning peak data and 0.7762 for midday. Furthermore, Figure 14 also shows that a linear relationship exists between the slew rate and the speed. The scatter plots are also used to compare the data from loop 1 and loop 2 at each double loop station. The plots confirm our intuition that each loop in the double loop station produces data with similar correlation between slew rate and speed. The plots of the morning peak downstream using loop 2 and the midday upstream using loop 1 are not shown as they are almost identical to the plots shown in Figure 14.

The next step is to model the relationship between slew rate and speed in order to predict and/or compute speeds. Given the scatter plots shown in Figure 14, the following simple linear model is postulated for the slew rate/speed relationship of the population:

Where:

| | | |
|---|---|---|
| $speed_i$ | = | dependent variable |
| $slew_i$ | = | independent variable, slew rate |
| $\_i$ | = | disturbance term |

In the context of linear regression,

$$\hat{s}peed_i = a + b\, slew_i$$
$$e_i = speed_i - \hat{s}peed_i$$

Where:

| | | |
|---|---|---|
| $\hat{s}peed_i$ | = | estimates of the speed |
| $slew_i$ | = | regressor, slew rate |

$a,b$ = parameters of regression

$e_i$ = residual

The following assumptions are made in order to perform linear regression. First, there is the assumption that no observations on $slew_i$ convey information about the expected value of the disturbance. In other words, the conditional expected value of the disturbance is equal to zero. This is a reasonable assumption since only the measurement errors and the random vehicle fluctuations contribute to the disturbance. The random vehicle fluctuations are the result of different driving behavior and vehicle mechanics. Second, the assumption of homoscedasticity is made. Last, the disturbances of the slew rates are assumed to be uncorrelated. The last two assumptions are also reasonable since there is nothing in the loop resonant circuit theory to suggest that variance is not constant across slew rates and that disturbances are correlated. These assumptions are supported by residual tests, and test outcomes are reported in the results section.

Least square estimation, which tries to minimize the sum of square residuals, is used to determine the parameters $a$ and $b$. The solution of the following normal equations yields the parameters of the regression model.

$$a\,n + b\sum_{j=1}^{n} slew_j = \sum_{j=1}^{n} speed_j$$

$$a\sum_{j=1}^{n} slew_j + b\sum_{j=1}^{n} slew_j^2 = \sum_{j=1}^{n} slew_j\ speed_j$$

Speed can then be predicted or computed for a vehicle by using the linear regression model and a given slew rate for that vehicle.

An interesting experimental concern arises when the standard error of $b$ is examined in the following equation

$$standard\ error\ \_\ \frac{\sigma}{\sqrt{n}} \bullet \frac{1}{s_{slew}}$$

(Wannocott, 1990):

The above equation implies that by increasing $S_{slew}$, the standard error of $b$ can be reduced. This suggests that one might want to collect the regression data by driving control vehicles over the loops with as wide a spread of slew rates as possible. However, this approach is a costly approach that detracts from the ease of implementation of the

proposed speed computation system. Consequently, only data from naturally occurring traffic is used for calibrating the proposed system.

### 3.3.4 Derivation of Ground Truth

The ground truth for individual vehicle speed is derived by using double loop data. Both digital and analog detector outputs were obtained during the vehicle waveform data colleciton. Double loop speeds that are computed using digital outputs can have typical errors of between 3% and 5% for commonly observed vehicles such as cars and pickups (Woods et al. 1994).

Pursula et al. (1989) found that the standard error of the speeds measured with analog waveforms was only one third of the error of the speeds with the traditional digital output from thresholds. This measurement of vehicle speed was determined by using the 50% amplitude point of the leading edge of the waveforms from loop 1 and 2 (Pursula et al. 1994). Thus, this technique is used in deriving the ground truth.

Figure 15 illustrates the double loop speed computation process. In this figure, the first waveform corresponds to the first loop in the speed trap, and second waveform corresponds to the second loop. For each waveform, the front edge is linearized, and the 50% point is determined and shown as a circle in the figure. The vehicle travel time is the difference between the time corresponding to the first circle and the second circle. Since the distance between the double loops is known, the speed is determined by dividing this distance by the travel time.

An alternate method that requires less computation is to use the peak of the waveforms. Waveform peaks are shown as asterisks in Figure 15. This method is less accurate since a waveform can have a plateau instead of a single peak. In fact, the example in Figure 15 exhibits such inaccuracies.

Regardless of which double loop speed computation method is used, there is some error associated with the measured speeds. More precise instrumentation composed of infrared beam curtains or high precision Doppler radars could yield a more accurate ground truth, but the cost of these devices prohibited their use for this research. Therefore the inaccuracy of the ground truth could have contributed to the error in the research results.

### 3.4 Results

First, the results from the linear regression will be shown. Then comparisons will be made with other single loop estimation methods. The sensitivity of the regression parameter with respect to the calibration size will be analyzed, and other model form possibilities will be discussed. In the results section, the term calibration is used to describe the process of estimating regression parameters.

The downstream morning peak dataset was divided into 300 vehicles for calibration, and the remaining 281 for testing. Linear regression was performed by using the first 300 vehicle waveforms from the second loop only, so an additional 300 vehicle waveforms from the first loop are also available for testing. The regression coefficient as well as several measures that are commonly included in regression analysis are listed in Table 1. The t-statistic shows that all coefficients are significant. The $R^2$ value confirms that a large fraction of the variance of the speed can be explained by the slew rate. The standard error shows that about two-thirds of the residuals will lie between -1.90m/s and +1.90m/s. The large value for the slope is due to the fact that the units of the independent variable is in term of % inductance change per millisecond.

Some analysis was performed on the regression residuals in order to validate the normality assumptions of the error term (_) and to verify that the error terms are not correlated. The error term is assumed to be distributed *N(0,_ $^2$)*, which means that it is normally distributed with zero mean and constant variance. Figure 16 shows the histogram of the residuals along with the table of descriptive statistics. The histogram and the statistics both show that the distribution of the residuals do not deviate significantly from normal, and the expected value of the distribution is almost zero. In order to test for heteroscedasticity, hypothesis testing is performed using the following null and alternate hypotheses:

$$H_o : \sigma_i^2 = \sigma^2, \forall i$$
$$H_1 : any\ \sigma_i^2 \neq \sigma^2$$

The application of White's heteroscedasticity test (White 1980) produced a small F-value of 0.6172, which means the null hypothesis cannot be rejected and the errors are homoscedastic. The Durbin-Watson statistic was 1.655 which shows only small evidence for autocorrelation, thus the model is not adjusted for time-ordered effects.

Table 2 shows the results comparing three different single loop speed computation methods. The test data were composed of 281 vehicles from the downstream morning peak data. The first column, labeled waveform speed, is the speed computed by the approach of using inductive waveform slew rates. The second column, labeled unbiased

speed, is the speed computed in the conventional fashion by using an unbiased estimate of the mean effective length (length of vehicle and detector). The estimated effective length was found to be 4.83 meters for the downstream morning dataset. This length is divided by the loop traversal time of the vehicle to obtain unbiased individual vehicle speed. The third column, labeled biased speed, is the speed computed by using a commonly assumed effective length of 6.55m (21.5ft) (Arendonk, 1996). An assumed effective length is commonly used by transportation agencies, since it does not require the sampling of vehicle lengths for estimating a sample mean. The data from the second loop of the speed trap is used for testing all three speed computations.

The results from Table 2 show that the waveform speed algorithm performed better than other conventional speed computation methods. The waveform speed was more accurate and shows less variability than the other two approaches. A value of 8.7% standard deviation for the unbiased speed computation error is not surprising, since this standard deviation is a function of the distribution of vehicle lengths. In locations where the traffic is more homogeneous in term of vehicle type for all times of the day, the unbiased speeds is expected to be much more accurate and to exhibit less variability than the results from Table 2. The biased speed shows a significant average error of 36.9%, since a biased effective length is assumed. This result shows that if an effective length which does not reflect the traffic characteristics of the particular location is assumed, then significant speed computation error will result.

In order to test the transferability of the calibrated algorithm and regression coefficient, speeds were recalculated using the vehicle waveforms from the first loop instead of the second loop. In other words, the second loop waveforms are used for calibration, while the first loop waveforms are used for testing. The results in Table 3 show the average error and the standard deviation of error increased only slightly when using testing data. Table 3 presents some evidence for the transferability of the calibrated algorithm.

In order to further verify the transferability of the calibrated algorithm, testing was performed using the vehicle waveforms from a different location recorded at a different time of the day. This dataset was recorded at the upstream site during midday. The results in Table 4 reaffirms the robustness of the algorithm. The average error remained the same while the standard deviation of error increased only slightly. It is interesting to note that the unbiased speed, computed using the unbiased mean effective length of this dataset, shows less error than the morning dataset. This result reflects the more homogeneous midday traffic that contains less truck traffic and more lunch time passenger vehicles.

The sensitivity of the regression parameter with respect to the calibration size and the associated average estimation errors are shown in Figure 17. Figure 17a shows that the regression slope fluctuates when less data is used for calibration, but the value levels off after 300 vehicles are used. This is the reason for using a calibration dataset size of 300 vehicles. Figure 17b shows the sensitivity of the average prediction error using a test data size of 231 vehicles. In terms of average prediction error, errors of around 7% are obtained after the calibration size is larger than 25 vehicles. However, regression theory shows that a larger variability in the independent variable leads to smaller standard errors in the residuals; therefore, a more conservative calibration size such as 300 vehicles will most likely contain more variability. Regression can also be accomplished by selecting a small set of vehicles that have a wide range of speeds, but such a set is not contiguous in terms of arrival times and does not lead to real-time calibration.

Table 5 shows the regression results of using other models forms to describe the relationship between slew rate and speed. The t-statistic shows that some coefficients of these more complicated model forms were not statistically significant. The $R^2$ values and the standard errors of regression are all similar between these model forms and the linear model. Also Figure 6 presents a strong graphical evidence for the use of linear regression. Therefore the simpler linear model is adequate for predicting vehicle speeds.

### 3.5 Conclusion

This chapter presented a new methodology for computing vehicle speeds using single loops. The inductive waveform slew rates were extracted, and a linear regression model was used for deriving speeds from slew rates. Data collected from Alton Parkway in Irvine, California, showed that this method could perform better than other methods of computing speed. One main advantage this method has over other methods is the fact that the accuracy of predicting speeds is not a function of the distribution of vehicle lengths. Another advantage, is the robustness of the method which was shown to be temporally and spatially transferable. This method requires very little computing power and cost to implement. The simplicity of the methodology leads to uncomplicated real-time implementations for traffic management and control purposes.

The utilization of the current single loop infrastructure avoids costly road closures and equipment associated with the cutting of double loops. In many cities and states, this infrastructure is extensive and can produce speed information for different Intelligent Transportation System needs. However, double loops or other detection systems are still necessary if high accuracy in speed computation is required.

Local accelerations can be computed by using this method if double loops are available. The local accelerations are simply the difference between the speed computed from the first and second loops in a speed trap. The local

accelerations can be a valuable input for congestion monitoring and incident detection algorithms. No acceleration results were presented because there was no ground truth available for validating results.

# CHAPTER 4 VEHICLE CLASSIFICATION

## 4.1 Introduction

Vehicle classification data is a valuable form of transportation data that can be used in many areas of transportation. One particular example of a vehicle class that is useful to be monitored is trucks. Trucks and other oversized vehicles have distinctly different performance characteristics than passenger vehicles. Trucks on the average travel at slower speeds, occupy more road space, have longer maneuvering times, have longer braking distances and times, and are sometimes lane restricted. In terms of traffic flow considerations, an accurate measurement of trucks on the road will lead to more accurate modeling and simulation of real world conditions. The assumption of uniformity of vehicle characteristics is a contributor to unrealistic modeling of real networks. The ability to convey and predict traffic conditions accurately on the roadway will also lead to improved efficiency through traffic control strategies. Because the speed differential between trucks and cars is usually significant, and also because trucks are much larger than passenger vehicles, having vehicle classification data can help safety research and implementation. Heavier vehicles like trucks also contribute disproportionally to the deterioration of pavements. Knowing the actual number of trucks traveled on a roadway can help estimate the life of the current road surface and assist in the scheduling of maintenance.

Another example of a vehicle class that is useful to be detected is light vehicles (LTV's). Some issues involving LTV's include the safety characteristic of such vehicles and car following behavior resulting from a higher driver field-of-view. The National Highway Traffic Safety Administration (NHTSA) reports that rollover crashes are one of the most significant safety problems for all classes of LTV's, especially light trucks (pickups, sport utility vehicles, and vans). NHTSA reports that rollovers resulted in an average of approximately 9000 fatalities per year or about thirty percent of all LTV fatalities from 1992 through 1996. Even though LTV's are in 68 percent as many crashes per registered vehicle as are passenger cars, LTV's are in 127 percent as many rollover crashes per registered vehicle.

Examples of applications with other vehicles classes also abound. Traffic signals can be pre-empted or extended when a bus or an emergency vehicle is detected. Automatic vehicle classification can be used for setting fees on toll roads. Vehicle class information can also help traffic enforcement agencies in maximizing their resources. Obtaining an area-wide assessment of traffic vehicle classes can help agencies estimate more accurately the types and amounts of pollution emitted by vehicles. Vehicle class information also allows the analysis of the effects of the increase in certain vehicle classes such as the growing percentage of sports utility vehicles (SUV) in the United States.

## 4.2 Review

There has been fertile research in the analysis and use of inductive signatures for transportation data collection both in the United States and abroad. Böhnke and Pfannerstill (1986) discussed the use of inductive signatures and Karhunen-Loeve transformation in reidentifying vehicle sequences. Kühne (1991) in cooperation with other researchers has published several reports of section measure instrumentation for obtaining inductive loop vehicle signatures. A freeway control system using a dynamic traffic flow model and vehicle reidentification technique was published by Kühne. Another system discussed by Kühne and Immes (1993) detailed a freeway control system using section-related traffic variable detection. Pursula and Pikkarainen (1994) used a seven vehicle class scheme for classification using double inductive loop signatures and self-organizing feature map. Sun et al. (1998, 1999a) describe a travel time and density measurement system using inductive loop signatures. Sun and Ritchie (1999b) used inductive signature slew rates to derive individual vehicle speeds from single loop detectors, as described in the previous chapter.

In terms of vehicle classification, there has been research using several detector technologies. Wei et al. (1996) used video classification and a backpropagation artificial neural network for deriving three vehicle classes. Yuan et al. (1994) also used video images and a hierarchical classification algorithm to derive six vehicle classes. Nooralahiyan et al. (1997) used acoustic signatures and a Time Delay Neural Network to derive four vehicle classes. Lu et al. (1989) used infrared detector and the k-nearest neighbor method for deriving four vehicle classes.

## 4.3 Methodology

The process of classifying vehicles can be divided into two phases: feature extraction and classification. The feature extraction portion seeks to extract the salient components of inductive signatures that would sufficiently differentiate vehicle classes. In order to avoid redundancy, each vector would contain different information. This is similar to the process of deriving a basis in linear algebra. In a likewise fashion, the goal here is to find an orthogonal set of vectors that would span the pattern space of possible vehicles signatures. Since this classification system is developed with future real-time implementation in mind, issues such as the cost of extraction, storage requirements, and communications bandwidth are of importance in addition to the classification rate.

The heuristic algorithms presented in this chapter use select feature vectors that were obtained from processing the inductive signatures. The classification phase involves the use of a heuristic, or a combination of several discriminant functions processed sequentially.

One advantage of this heuristic approach is the reduction of data and communication requirements by using processed feature vectors. A fixed number of feature vectors will be inputs to the classification algorithm instead of

entire signatures. Feature vectors that were considered include the vehicle electronic length, inductive magnitude, energy content, signature variance, signature skewness, signature kurtosis, Karhunen-Loeve transform coefficients of the signature, Discrete Fourier Transform of the signature, and number of maxima/minima of the signature. Only a subset of these feature vectors were used in developing the three heuristic algorithms as some feature vectors contained redundant information. Other feature vectors that were not used in the three heuristic algorithms presented here can possibly be used efficiently in other classification algorithms related to particular transportation applications.

Another advantage of the heuristic approach is that the sequential classification stages are explicitly defined. Therefore problems with a particular stage can be identified and corrected without having to rebuild a complete classification algorithm. The sequential aspect of the algorithm also results in efficient computation since the feature space is reduced as the algorithm proceeds sequentially.

The following paragraphs discuss the classification portion of the heuristic algorithm. One approach in pattern recognition algorithms is to use a nonparametric decision theoretic approach. In this approach, no assumptions of class distributional forms are made. If each signature is considered to be a pattern in the pattern space, then signatures pertaining to different vehicle classes will fall into different regions of this pattern space. A separating surface can then be defined to differentiate between the different classes. In one-dimensional space, the decision surface is a point that divides the linear pattern space as seen in Figure 18 (Bow, 1992).

Assume that the use of each feature vector is a one-dimensional discrimination problem, then vehicle classification can be performed by using a single feature vector. However, since the feature vectors are not completely correlated or redundant, multiple feature vectors can be combined to improve classification rate and to increase the number of classification categories. Conceptually, this is illustrated in Figure 19 in which heuristic classification trees use several feature vectors to arrive at seven separate classes. These heuristic classification algorithms which combine multiple feature vectors is the approach undertaken for this research. Figure 19 shows a hierarchical structure that is similar to the hierarchical structure of syntactic pattern decomposition schemes and is equivalent to a piecewise linear discriminant function.

### 4.3.1 Training Methodology

The training of the heuristic algorithms involves the determination of the optimum discriminant bounds of the discriminant functions used in the heuristic tree. The objective in training the heuristic algorithm is to minimize the number of misclassifications or

$$\min_{\tilde{b}} \sum_{j=1}^{N_v} \delta(\tilde{b}, \tilde{x}_j), \quad \forall i$$

where $\delta(\tilde{b},\tilde{x}j) = \begin{cases} 1, \text{ if } x_j \text{ is classified correctly} \\ 0, \text{ if } x_j \text{ is classified incorrectly} \end{cases}$ , $N_v$ is the number of training vectors, $\tilde{b}$ is a vector of boundaries that define the decision surfaces. Note that each training vector derived from a single vehicle signature is composed of multiple feature vectors. In other words,

$\tilde{x}_j = x_{j1}, x_{j2}, ..., x_{jN_f}$

and $N_f$ is the number of feature vectors per vehicle signature.

This optimization problem can be reformulated as a hierarchical multi-objective optimization (or lexicographic optimization) problem. Instead of finding the components of $\tilde{b}$ simultaneously, a staged approach is taken to find each component of $\tilde{b}$ sequentially. At each stage, a separate feature vector is considered, and the decision surfaces are determined. A well-known minimization technique called golden section search was used for each optimization stage. The optimization is complete when Pareto optimality is achieved. At such an instance, it is not possible to move feasibly so as to increase one of the objectives without decreasing at least one of the others (Steuer, 1986).

Golden section search was used because the only critical property for applying this method was for the objective function to be unimodal (Luenberger, 1989). Since the objective function is derived heuristically it has no mathematical functional form, thus gradient search methods can not be used. The unimodal property is satisfied when the distributions of the feature vectors are unimodal. Figure 20 illustrates a simple example of unimodal feature vector distributions for two classes. This property needs to be checked before a feature vector is used. If a distribution is multi-modal, then an inferior solution can result from searching and finding a local minimum. Figure 21 gives examples of the unimodal objective function from using the length feature vector which has a unimodal distribution.

#### 4.3.2 Data Description

The data set was composed of approximately 2000 vehicles of moderate flow traffic (1000 VPHPL). The data set included the inductive signatures and video ground truth of the vehicles. This data set was further reduced to 300 vehicles in order to contain a more uniform distribution of signatures across all vehicle classes. This avoids the problem of biasing any algorithm towards passenger cars since most vehicles were in that category. The manageable size of the data set allows detailed analysis of each vehicle signature and the examination of the causes for each individual misclassification. The field data were obtained from two freeway sites on the westbound SR-24 freeway in the city of Lafayatte in Northern California. By training and testing using data collected from different sites, the transferability of the algorithms was tested. Note that no calibration of the loops was performed between sites or within the multiple loops at each site. The distance between the two freeway sites was approximately 2 km (1.2 miles) long. At each detector station there were four lanes. Each data acquisition station was instrumented with video, inductive signature dataloggers, and speed trap dataloggers. Standard 1.82mX1.82m (6'X6') loops were used

at both stations. The data set was separated into a training set and a test set of roughly equal size. The number of vehicles in each of the classes was not equal, thus there were more vehicles in the first three classes than in the last four. The reduced data set contained the signatures of the vehicles along with their speeds, arrival time at stations, lane number, and the ground truth video. This dataset was composed of moderate flow traffic (~1000 VPHPL). The calibration of the algorithms was performed on the training data only.

### 4.4 Results

Three different heuristic algorithms were developed and tested. Conceptually, the three heuristics are illustrated in flowcharts in Figure 19. These three algorithms differ in the feature vectors that are used, in the order in which they are used, and in the number of discriminant surfaces per feature space. As seen in Figure 19, the first level discriminants used for the three algorithms were length, magnitude, and kurtosis. Algorithms one and two are more similar because they use multiple discriminant surfaces for the length feature space, while the third algorithm only makes binary decisions.

The purpose in presenting three algorithms is to show examples of how different feature vectors can be combined in various ways to produce classification algorithms. This research was not intended to promote a single algorithm nor to promote an optimum set of feature vectors for all applications. The three algorithms then are used to demonstrate the feasibility of using the heuristics for vehicle classification. For a particular ATMIS application, the heuristic algorithms can be modified to suit that application.

A vehicle classification scheme using seven vehicle classes was used for testing algorithms. This scheme is described in detail in Table 6. This scheme is chosen because it yields classes that can be adapted for several applications including pollution, safety, and traffic analysis. This scheme is also chosen because it targets vehicle classes that are not differentiable by using current techniques based on axle counting. For any particular application, the number of classes in the heuristic classification scheme can be decreased or increased to suit that application.

Table 7 shows the heuristic bounds used in each algorithm. These bounds were determined by using golden section search. The tolerance used in stopping the golden section search was for the distance between the outside bracket points to be smaller than 0.0005.

The overall classification rates from using heuristic 1 were very similar between the training and the test set as seen in Table 8. Algorithm 1 is heavily dependent upon the length feature vector, since the length is used as the top level discriminant and it is used to differentiate five categories. Even though length proved to be effective as a top level discriminant, its use was not sufficient to separate class 1 from class 2 or class 6 from class 7. The inductance magnitude was used to separate minivans and SUV's of the same length, and skewness was used to separate trucks

and buses of the same length. One advantage of using inductive signatures over length as an input to a classification system is the ability to separate vehicle classes among vehicles of the same length. The performance of algorithm 1 was good for all classes except class 5. This motivated the development of another algorithm that would maintain the overall classification rates while at the same time improve performance for class 5.

Heuristic 2 was developed by replacing length with magnitude as the top level discriminant. The basis for this decision was the fact that the inductance magnitude is approximately inversely proportional to the square of the height of the vehicle undercarriage from the loop. Therefore trucks and other vehicles with high undercarriage clearances would produce signatures with lower magnitudes. Even though algorithms 1 and 2 used the same feature vectors, the results were different as seen in Table 8. The classification rate for class 5 increased but classification rates for class 6 and 7 decreased. This was not surprising since class 5 and class 7 are closely related.

For heuristic 3, Table 8 gives the vehicle overall classification rate and rates by vehicle class. The overall classification rate of almost 90% demonstrates that there is potential in using heuristics for vehicle classification. The performance across all categories is more consistent than previous algorithms. The poorest performing category is class 4 which is composed of limousines. This category is problematic because even though limousines have inductive magnitudes that are similar to passenger cars, their lengths are similar to trucks.

The results of the test set shows that the classification rate went down slightly as compared to the training set. The individual class rates were also consistent across the board. The results of the test set again point to the potential of using heuristics for vehicle classification.

In Table 9, the results of individual classifications were tabulated. This is useful in analyzing both type I and type II errors in classification. If the null hypothesis is that the vehicle was correctly classified, then Type I error is the rejection of the null hypothesis when it is true and Type II error is not rejecting the null hypothesis when it is false.

### 4.5 Conclusion

The vehicle classification algorithms described in this chapter exploit the current inductive loop infrastructure by collecting inductive signatures. By using these signatures, surveillance capabilities are increased, one of which is the ability to derive vehicle classification data. These data can be used as inputs to various ITS strategies in order to improve the efficiency, safety, environmental sustainability, and maintainability of transportation networks.

The vehicle classification algorithms described in this chapter presented three different heuristics that combined different feature vectors in different ways to separate vehicle classes. These algorithms then are examples from which other heuristic algorithms could be developed for particular ITS applications.

One advantage of using the heuristic classification algorithm is the reduction of data transmission and storage requirements that results from using feature vectors instead of raw signatures. Another advantage is the sequential discrimination of the heuristic algorithm which reduces the feature space at each stage of discrimination. This staged procedure also has the benefit of allowing the fine-tuning of each stage (discriminant function) independently. As a result of the aforementioned advantages, these heuristic algorithms are suitable for real-time implementation.

This chapter also formulated a multi-objective optimization problem for training the heuristic algorithms. The training involves the determination of optimum discriminant bounds using golden section search.

The three heuristic algorithms produced encouraging results of 81%-91% overall classification rates. In addition, the individual classification rates were fairly uniform, especially for the third heuristic algorithm. These results demonstrate that the derivation of vehicle classification information from inductive signatures has great potential in ITS applications.

Because the classification schemes used by previous researchers differ, it is difficult to compare classification algorithms based on the classification rates alone. In a sense, different technologies yield classification schemes that are more suitable for the particular kind of signal that is detected. Consequently, it might be fruitful in the future to consider a combination of different technologies in order to optimize the classification for a particular transportation application. This becomes increasingly feasible as costs of detector technologies drop in response to demand and innovation.

# CHAPTER 5 REIDENTIFICATION ALGORITHM ENHANCEMENT

## 5.1 Vehicle Reidentification

Vehicle reidentification is based on a vector of features extracted from the raw vehicle signature, and other information such as vehicle speed and lane information. The feature vector should include salient components of the vehicle signature that would sufficiently differentiate vehicles. Therefore, vehicle reidentification is a discrete analysis based on a given set of feature vectors.

In this study, proposed feature vectors at both downstream and upstream detector stations were:

- Arrival time at each station
- Vehicle Speed
- Vehicle Length
- Lane Information
- Interpolated waveform ordinates
- Maximum magnitude of each waveform

Applying the concept of lexicographic optimization, a sequential approach to solving multi-objective optimization problems, vehicle reidentification was formulated as a five-level optimization problem by Sun et al (1999) as part of a previous PATH project (MOU 224). Feature restrictions were applied at each level to derive reasonable vehicle subsets and to limit the search space for matching vehicles. Minimizing mismatches between feature vector pairs denotes the "optimization" on any given objective. However, the previous vehicle reidentification algorithm was restricted to a freeway case and only considered "regular" vehicle signatures. In this study the algorithm was modified to enhance its performance under different study sites, specifically including surface streets, and to address so-called "irregular" vehicle signatures.

## 5.2 Irregular Signatures

"Regular" signatures are referred to as those that have two complete waveforms with similar maximum magnitude from each waveform, as referred to in section 2.3. However, irregular signatures sometimes appear due to traffic conditions, vehicle movement across the loops, and loop corrosion. To address these irregularities, "pre-processing" of the data is required. This is also related to obtaining 100% correct vehicle counts at each station because by accounting for irregular signatures more accurate volume counts can be obtained. Several types of observed irregularities are described below. Turning movement signatures are presented separately in section 5.3.

### 5.2.1. Partial Overlap Signature

As shown in Figure 22 and Figure 23, this irregularity is related to the front loop waveform. Short space headways were the main reason for this irregularity. The front or first waveform of Figure 23 contains part of the front loop waveform of Figure 22. If the headway was excessively short, then the signature will look more likely Figure 23. The modified algorithm captures these signatures as "irregular" ones and transforms them into regular signatures based on the provided vehicle signature features.

### 5.2.2. Tailgating Vehicle vs Vehicle with Boat

Tailgating vehicles often produce a signature that has two vehicles completely contained within a single signature, as shown in Figure 24. This also results in an incorrect vehicle count – by counting one vehicle instead of two vehicles. Pre-processing such signatures can address this irregularity and provide differentiation from vehicles towing a trailer such as the "vehicle with boat" signature shown in Figure 25, which looks similar to this irregular case.

## 5.3 Turning Movement Filtering

Signatures of turning vehicles show typical characteristics, which are fairly specific depending on the loop layout. As described in Figure 2, at the Alton/ICD intersection study site, the downstream loops were located right after the intersection and most of the turning vehicles hit the loops at an angle. Consequently, many turning vehicles did not pass over both loops completely but instead hit one or both loops partially. As a result, the difference in the maximum magnitude between front loop and back loop waveform was substantial compared to through movement vehicles. This fact is clearly illustrated in Figure 26. Figure 27 shows the distribution of maximum magnitude differences between front and back loops based on collected downstream station data on February 25th, at the Alton/ICD intersection. In most cases of through movements, the maximum magnitude difference range was from 0 to 50. But for the turning vehicles, the maximum magnitude difference varied from 0 up to 680. Therefore, even though traffic signal information was not provided, by reading the maximum magnitude difference, the algorithm was able to adequately classify arriving vehicles according to their upstream origins.

Since the maximum magnitude of each waveform is one of the features in our vehicle reidentification algorithm, these irregularities are categorized separately to apply different weight values in the vehicle reidentification algorithm. Also, effective turning filtering is essential to appropriately limit the search space for upstream vehicles and reduce the mismatching rate. Reidentification is meaningless if the algorithm tries to match a downstream vehicle with an upstream vehicle set that does not include the "true" corresponding matching vehicle. This problem

is addressed in the turning movement filtering routine. For example, if the downstream vehicle is determined to have turned left, then only the corresponding left turning upstream vehicle set (vehicles turning left) will be considered in the algorithm. Consequently, turning filtering will lead to a lower mismatching rate. This procedure also saves algorithm execution time, which is one of the core requirements for real-time application. Provision of signal phase information in the future will likely lead to improved turning filtering results as well.

### 5.4 Sequence Consideration

Vehicles often move in platoons, especially in signalized networks, and this platoon structure is often maintained as vehicles pass through the network, unless the O-D of vehicles in the platoon is changed. By incorporating this concept in our vehicle reidentification algorithm, some mismatching problems can be avoided. The algorithm keeps the upstream sequence order for each downstream vehicle once it is reidentified. Then, for the next reidentified downstream vehicle, the algorithm compares the matched upstream vehicle sequence with the previous downstream vehicle. If the upstream sequence is not consistent with the downstream sequence, then the algorithm automatically declares a "miss". This avoids matching a downstream vehicle with one upstream that is well removed from its expected platoon or sequence order. Sequence consideration is the same as imposing one more restriction in our reidentification process. Adding more restrictions probably yields more precise matching results, but there may also be a trade-off in giving a lower matching rate. However, it is more believed preferable to provide less but more reliable information rather than more but less accurate information.

The modified vehicle reidentification procedure is described in Figure 28. The derived features at each algorithm step are on the right side of the figure. Half of the dataset from each study site was trained for the calibration of the optimal weight value for each feature in the matching procedure. The results from applying the modified reidentification algorithms are presented in the next Chapter.

# CHAPTER 6 RESULTS FROM MODIFIED REIDENTIFICATION ALGORITHM

## 6.1 Introduction

Two datasets were used to test the reidentification algorithm performance. Section 6.2 presents algorithm results from the Alton Parkway arterial dataset. An improved matching rate from the modified algorithm is described in this section. Reidentification results from the Alton/ICD intersection are presented in section 6.3. For both datasets, algorithm outputs based on single loop speed and double loop speed are also compared.

There are three categories in the reidentified result for each downstream vehicle. The correctly matched vehicle is the case when the algorithm correctly matched the upstream vehicle, verified by video ground truth, for the downstream vehicle. An incorrectly matched vehicle corresponds to the case when the algorithm output is different from the actual vehicle pair. The case when the algorithm cannot declare a matching upstream vehicle for the given downstream vehicle result is categorized as a missed vehicle. This happens when none of the vehicles in the upstream search space satisfies the algorithm restrictions (as well as when the restrictions are set too strictly). This might lead to a lower matching rate but at the same time, the algorithm result is more reliable than one derived from looser restrictions.

## 6.2 Alton Parkway

### 6.2.1 Addressing irregularities

Table 10 shows the reidentification result using the Alton Parkway AM dataset. The reidentification algorithm addresses the irregular signatures discussed earlier. Except for bus, the correct matching rate for each vehicle type is above 78 %. Especially for the truck and trailer case, a 100 % matching rate is achieved since these signatures have more distinguishable features. The shaded box in Table 10 indicates, as an example, the number of passenger cars at the downstream station that were mismatched as an upstream pickup truck by the algorithm. Even though the features of the single bus in this dataset were quite distinct, its slow travel time didn't satisfy the time restriction (or time window) at the first level of the algorithm. Therefore, the bus was classified as a missed vehicle in this result.

Travel time is regarded as the most significant parameter for Advanced Transportation Management and Information System. In this regard, the vehicle reidentification algorithm shows promising results as a way to obtain section travel time. A 100% matching rate is not necessarily required for the section travel time calculation as the section travel time will be the average value during each interval. Figure 29 shows the results obtained for an

interval of 60 second. The average percentage error was slightly different according to the sampling interval but the error was less than 3% in all cases, as shown in Figure 30

In this study, section density refers to the number of vehicles remaining in the section at the end of each interval. The results shown in Figure 31 indicate that the matched section density tracks the correct section density closely. As shown in Figure 32 the average percentage error was less than 5% in all cases.

### 6.2.2 Using Single Loop Speed vs Double Loop Speed

A small dataset of 182 vehicles from Alton Parkway was used to evaluate single loop speed application in the reidentification algorithm. Figure 33 shows the relationship between speed from double loop, which is regarded as true speed, and speed derived from a single loop. The average error was 8.9%. Vehicle speed is essential to get vehicle length. Since vehicle length and speed are both one of the reidentification features, small errors in speed and length may yield different vehicle matching results. As shown in Table 11, the reidentification result using single loop speed is very encouraging even though it was based on a small dataset  Overall, the matching rate decreased by only 3.5% from 73.1% to 69.8%.

## 6.3 Intersection of Alton Parkway and Irvine Center Drive

### 6.3.1 Reidentification With Only a "Through" Movement

For the Alton Parkway and Irvine Center Drive (Alton/ICD) intersection study site, only one through movement was considered due to the 2070 controller limitations, as mentioned earlier.

Table 12 shows the collected data on February 25th, 2000. If the vehicle was detected at lane 1 upstream and at downstream lane 1, then this vehicle is categorized as "matching at downstream" in the upstream column and "matching at upstream" in the downstream column. In our dataset there were 113 vehicles in this category. Vehicle reidentification was performed only for this category since there were no upstream or downstream datasets for the remaining categories.

The downstream station at the intersection contains three origins – through, left and right movements. Vehicle origins for vehicles arriving at the downstream station were identified through the "turning filter" routine in the reidentification algorithm.

The maximum travel time and average travel time were 100 seconds and 42.05 seconds, respectively, in our dataset. By assuming a 90 second cycle length, most of the vehicles were able to pass the intersection within one cycle

As shown in Table 13, the overall reidentification matching rate for this dataset was over 84% for all vehicle types. 8 passenger cars were mismatched with other passenger cars. This is reasonable since many passenger cars share similar feature vectors. However, it is hard to conclude that the algorithm result will be similar under any traffic conditions. More extensive study using various datasets is required to evaluate the algorithm performance. But the result using this small dataset provides a promising approach for intersection system performance analysis.

Figure 34 shows the relationship between true travel time and travel time from the algorithm. The points that follow closely the 45 degree line correspond to correctly matched vehicles. Points that deviate from this line are incorrectly matched pairs. We can see that the algorithm result tends to estimate quite well true travel time. Average section travel time from the algorithm was 45.30 sec and the percentage error was 7.8%. A more appropriate time window restriction based on signal information would likely solve this lower this error.

### 6.3.2 Using Single Loop Speed vs Double Loop Speed

As in section 6.2.2, single loop speed was applied to evaluate its impact on algorithm performance. The correlation between single loop speed and double loop speed is shown in Figure 35. The average percentage error was 11.5%, which is higher than in the previous section 6.2.2. This error rate impacted the reidentification performance, as shown in Table 14. Table 14 shows that the matching rate changed from 84.1% to 71.7%, a 14.7% decrease, but still a good matching rate.

# CHAPTER 7 CONCLUSIONS

## 7.1 Conclusions

With the existing widespread use of inductive loop detectors (ILDs), Intelligent Transportation Systems (ITS) have a constant source of information on traffic system conditions. However, ILDs typically provide only point measures of traffic characteristics such as volume, occupancy, and depending on the loop configuration, local speed, which are inadequate for many ITS applications. If these detectors could be used in a "smarter" way, more useful information could be obtained for important ITS applications in traveler information and route guidance systems, congestion monitoring and incident detection, and traffic control via freeway ramp meters, surface street signals and changeable message signs. One technique to obtain significantly more information from ILDs is to utilize the vehicle waveforms that are produced when each vehicle passes over a loop. Such waveforms are essentially "signatures" that can be reidentified at downstream stations, and yield more useful information such as real-time section travel times, section speed, and section density, as well as vehicle classification and origin-destination data.

In this project (MOU 336), an initial phase of a field implementation was accomplished of the results of a previous research project (MOU 224), in which a vehicle reidentification algorithm based on loop signature analysis was developed using freeway traffic data. This algorithm was extended to non-freeway cases, initially using a section of 2-lane major arterial in cooperation with the City of Irvine, California. The technique was enhanced to address problems such as "irregularities" in vehicle signatures associated with trucks, tail-gating vehicles and erroneous counting of vehicles, with the objective of obtaining 100% correct counts at each station.

The enhanced algorithm was also applied to a major specially instrumented signalized intersection in Irvine, California to demonstrate acquisition of data for real-time congestion monitoring, incident detection and level of service measurement. The initial application was for through vehicles on one approach. In order to achieve more reliable vehicle reidentification results, additional routines for vehicle movement filtering at the downstream station were applied. Reidentification results based on an initial dataset showed an encouraging matching result of 84.07% overall, for individual vehicles. On-line real-time vehicle reidentification operation (for the same approach, but for all three departure movements: left, though and right), and a Graphical User Interface for the algorithm are being developed under another PATH project (MOU 3008).

Speed estimation from a single loop signature was one of the applications investigated in detail. For several study sites, the vehicle reidentification matching rates, using speed estimated from a single loop, were only slightly lower than for double loops. In another detailed application (using freeway data collected in a previous PATH project, MOU 224), vehicle classification using a Backpropagation Neural Network showed an 80 % classification rate overall for all vehicle types. Heuristic approaches to vehicle classification also demonstrated good results.

This study has significantly advanced a new framework based on conventional inductive loop detectors that has now been shown capable of estimating freeway, arterial and intersection measures of traffic performance, including section speed and travel time, section density, and vehicle travel time through a signalized intersection, among others. It has been shown that quite accurate estimates of vehicle speed can be obtained from single inductive loop detectors instead of the double loops previously used in this research, greatly expanding the potential for application of loop-based vehicle reidentification techniques. The potential was also demonstrated for real-time derivation of vehicle classification information from inductive signatures.

In summary, this research has shown that low-cost enhancements to the preexisting traffic surveillance infrastructure can be an economically attractive means of obtaining expanded and more accurate traffic performance and travel information. Applications of such vehicle reidentification concepts show encouraging results for potential direct use in providing network-wide travel information.

**REFERENCES**


1. Athol, P. (1965) "Interdependence of Certain Operational Characteristics Within a Moving Traffic Stream." Highway Research Record 72. Pp. 58-87. HRB. National Research Council. Washington, D.C.
2. Arendonk, J. (1996) "A Comparison of Real-Time Freeway Speed Estimation Using Loop Detectors and AVI Technologies.", Southwest Region University Transportation Center. Compendium: Graduate Student Papers on Advanced Surface Transportation Systems. Texas Transportation Institute. Texas A&M, College Station. Pp. J1-J40.
3. Bahler, S.J., Minge, E.D., and Kranig, J.M. (1998) " Field Test of Non-Intrusive Traffic Detection Technologies." Preprint. Transportation Research Board 77th Annual Meeting. January 11-15. Washington, D.C.
4. Böhnke, P. and Pfannerstill, E. (1986) "A System for the Automatic Detection of Traffic Situations." ITE Journal. Vol. 56.
5. Bow, S.T. (1992) "Pattern Recognition and Image Preprocessing". Marcel Dekker, Inc. New York. Pp. 1-142.
6. Garrott, W.R., Howe, G.J., and Forkenbrock, G. (1999) "An Experimental Examination of Selected Maneuvers That May Induce On-Road Untripped, Light Vehicle Rollover". National Highway Traffic Safety Administration. Washington, D.C. July.
7. Hall, F.L., and Persaud, B.N. (1989) "Evaluation of Speed Estimation Made with Single-Detector Data from Freeway Traffic Management Systems." Transportation Research Record 1232. Pp. 9-16.
8. Hughes Aircraft Company and JHK & Associates. (1994) "Vehicle Detector Field Test Specifications and Field Test Plan." Task 4 Report for Detector Technology for IVHS. United States Department of Transportation. Federal Highway Administration. Washington, D.C. Contract Number DTFH61-91-C-00076.
9. Institute of Transportation Engineers. (1990) Traffic Detector Handbook. Washington, D.C.
10. Jacobson, L.N., Nihan, N.L., and Bender, J.D. (1990) "Detecting Erroneous Loop Detector Data in a Freeway Traffic Management System." Preprint. Transportation Research Board 69th Annual Meeting. January 7-11. Washington, D.C.
11. Klein, L. (1995) "Modern Detector Technology for Traffic Management." Presentation for the University of California, Irvine. February 28.

12. Kühne, R. D. (1991). "Freeway Control Using a Dynamic Traffic Flow Model and Vehicle Reidentfication Techniques". Transportation Research Record 1320. Pp. 251-259
13. Kühne, R. D and Immes, S. (1993) "Freeway Control Systems for Using Section-Related Traffic Variable Detection". Pacific Rim TransTech Conference, July 25-28, Seattle, Washington.
14. Luenberger, D.G. (1989) "Linear and Nonlinear Programming". Addison-Wesley. Reading. Pp. 198-200
15. Lu, Y. (1989) "Vehicle Classification Using Infrared Image Analysis". ASCE Journal of Transportation Engineering. Vol. 118. No. 2. March/April. Pp. 223-240.
16. Mikhalkin, B., Payne, H.J., and Isaksen, L. (1972) "Estimation of Speed from Presence Detectors." Highway Research Record 388. Pg. 73-83. HRB. National Research Council. Washington, D.C.
17. Nooralahiyan, A.Y. et al. (1997) "A Field Trial of Acoustic Signature Analysis for Vehicle Classification". Transportation Research-C. Vol. 5. No.3/4. Pp. 165-177.
18. Numerical Recipes Software. (1992) Numerical Recipes in Fortran 77 : The Art of Scientific Computing. Cambridge University Press.
19. PATH (Partners for Advanced Transit and Highways) (1997) "Workshop on Research, Development, and Testing of Traffic Surveillance Technologies." Richmond Field Station. California.
20. Provenza, J. (1985) "Loop Detector Systems." International Municipal Signal Association Journal, Volume XXII, March-April, Number 2, Pp. 5-7.
21. Pursula, M. and Kosonen, I. (1989) "Microprocessor and PC-based Vehicle Classification Equipments Using Induction Loops." Proceedings of the Second International Conference on Road Traffic Monitoring. IEE Publication Number 299. London. February 7-9. Pp. 24-28.
22. Pursula, M. and Pikkarainen, P. (1994) "A Neural Network Approach to Vehicle Classification with Double Induction Loops". Proceedings of the 17th ARRB Conference. Part 4. Pp. 29-44
23. Steuer, R.E. (1986) "Multiple Criteria Optimization: Theory, Computation, and Application". John Wiley & Sons. New York. Pp. 165-183, 196.
24. Sun, C., Ritchie, S., and Tsai, W. (1998) "Algorithm Development for Derivation of Section-Related Measures of Traffic System Performance". Transportation Research Record 1643. Pp. 171-180.

25. Sun, C., Ritchie, S., Tsai, K., and Jayakrishnan, R. (1999a) “Use of Vehicle Signature Analysis and Lexicographic Optimization for Vehicle Reidentification on Freeways”. Transportation Research Part C. Vol No . Pp
26. Sun, C. and Ritchie, S. (1999b) “Individual Vehicle Speed Estimation Using Single Loop Inductive Waveforms”. Forthcoming in American Society of Civil Engineers Journal of Transportation Engineering.
27. Taylor, S.S. (1972) "Inductive Loop Detector Functions." Department of Traffic, City of Los Angeles. Staff Report No. 53.08. February 4.
28. Wannacott, T.H. and Wannacott, R.J. (1990) Introductory Statistics. Wiley & Sons. New York.
29. Wardrop, J.G. (1952) "Some Theoretical Aspects of Road Traffic Research." Proceedings Instn. Div. Engrs., Vol. 1, No. 2. Pp. 325.
30. Wei, C. et al. (1996) “Vehicle Classification Using Advanced Technologies”. Transportation Research Record 1551. November. Pp. 45-50.
31. White, H. (1980) "A Heteroscedasticity-Consistent Covariance Matrix Estimator and a Direct Test for Heteroscedasticity." Econometrica, 48. Pp. 817-838.
32. Wilshire, R., Black, R., Grochoske R., and Higinbotham, J. (1985) Traffic Control Systems Handbook. Institute of Transportation Engineers. Washington, D.C. Report No. FHWA-IP-85-12. April.
33. Woods, D.L., Cronin, B.P., and Hamm, R.A. (1994) "Speed Measurement with Inductance Loop Speed Traps." Texas Transportation Institute. Research Report FHWA/TX-95/1392-8. Texas A&M. College Station..
34. Yuan, X. et al. (1994) “Computer Vision System for Automatic Vehicle Classification”. ASCE Journal of Transportation Engineering. Vol. 120. No. 6. November/December. Pp. 861-876.

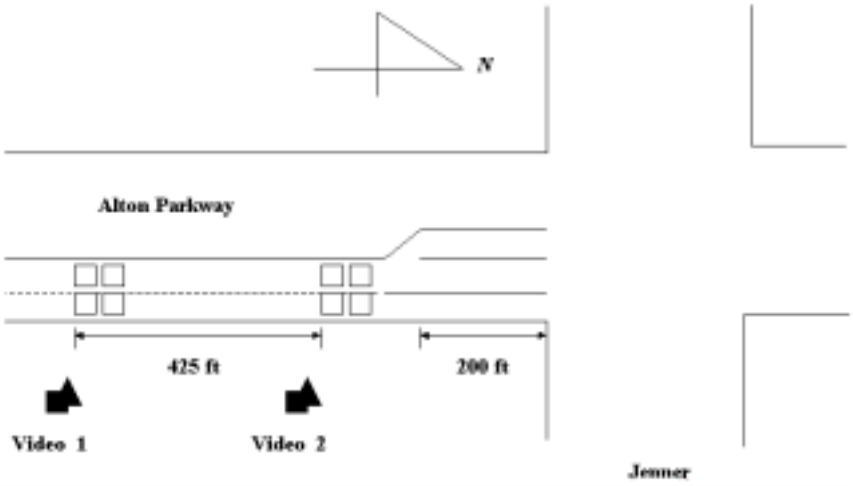


Figure 1 Alton Parkway Study Site

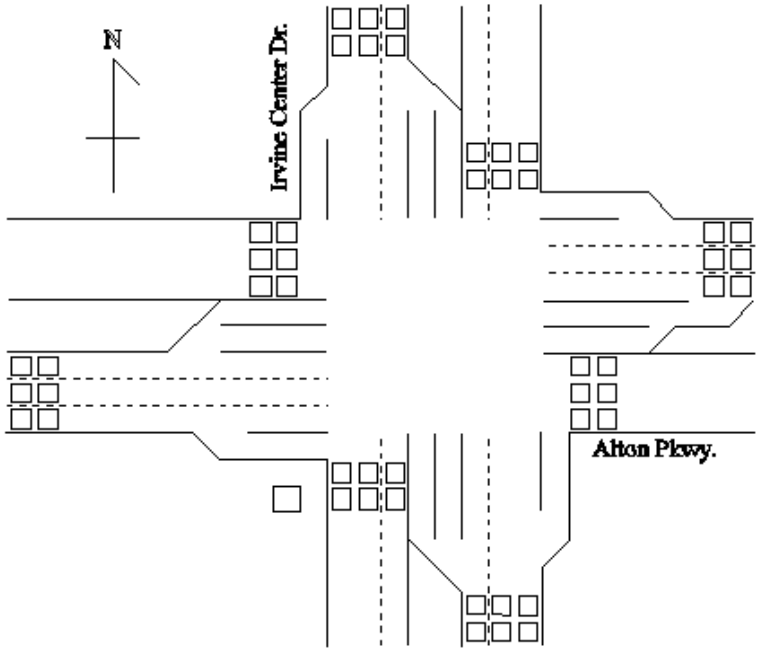


Figure 2 Alton/ICD Intersection Study Site

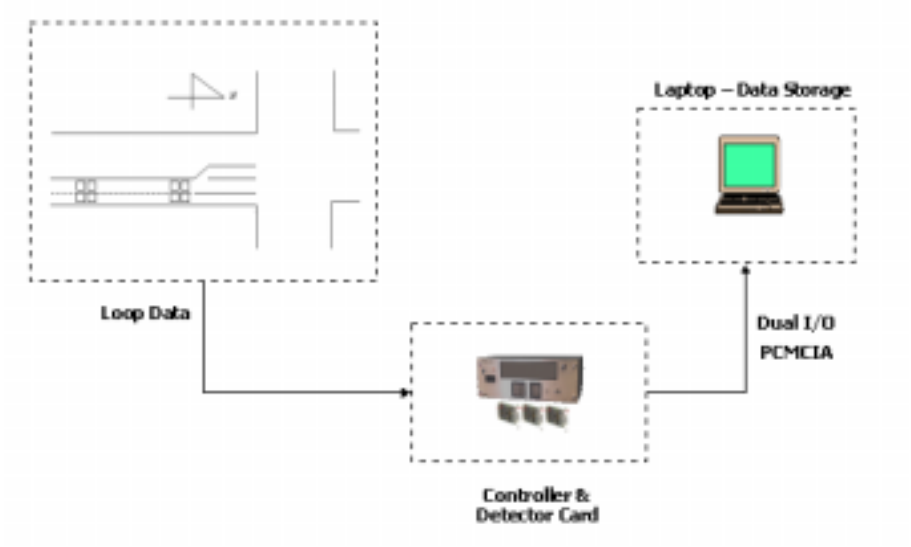


Figure 3 Alton Parkway Data Collection and Transmission Setup

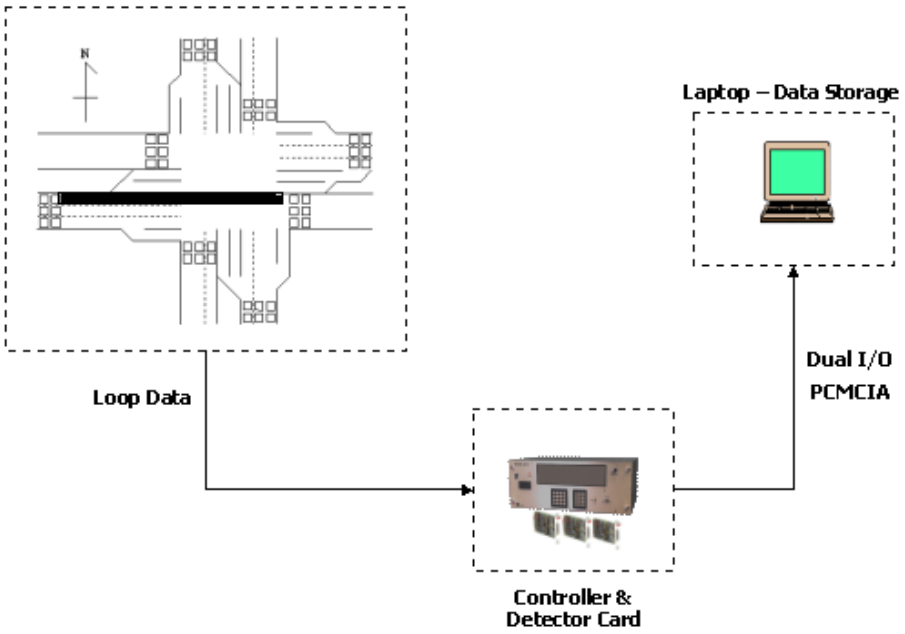


Figure 4 Stage One

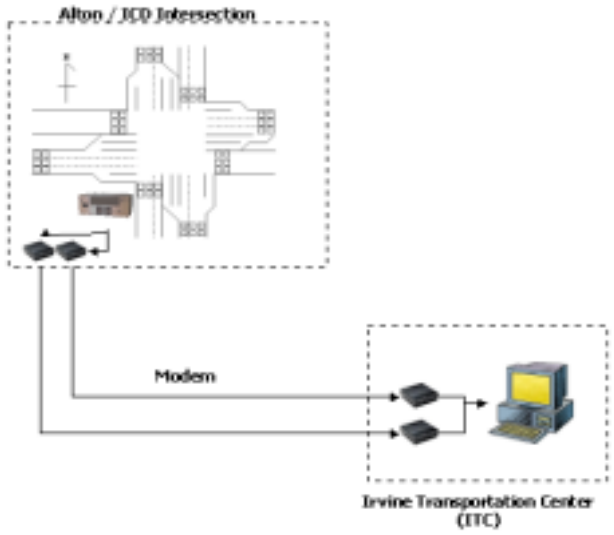


Figure 5 Stage Two

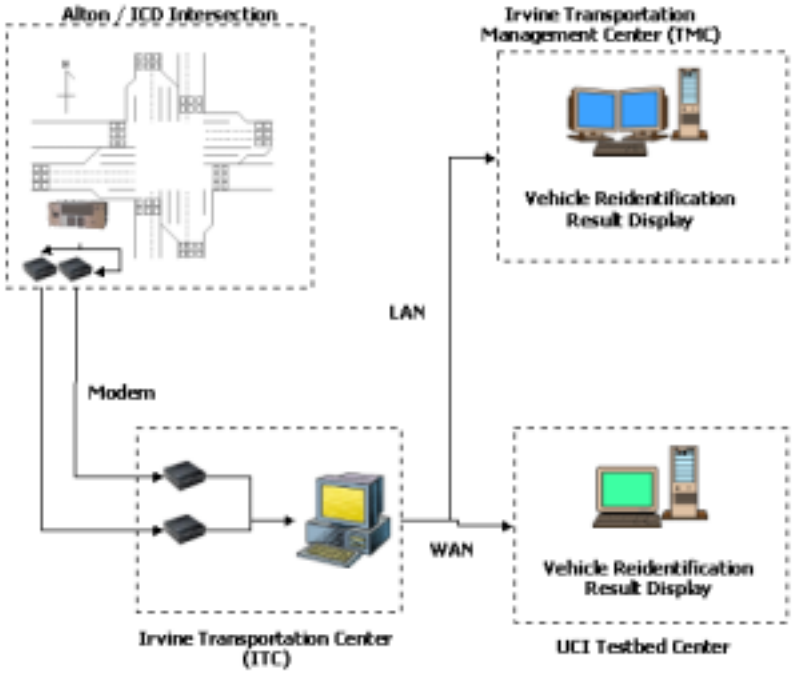


Figure 6 Stage Three

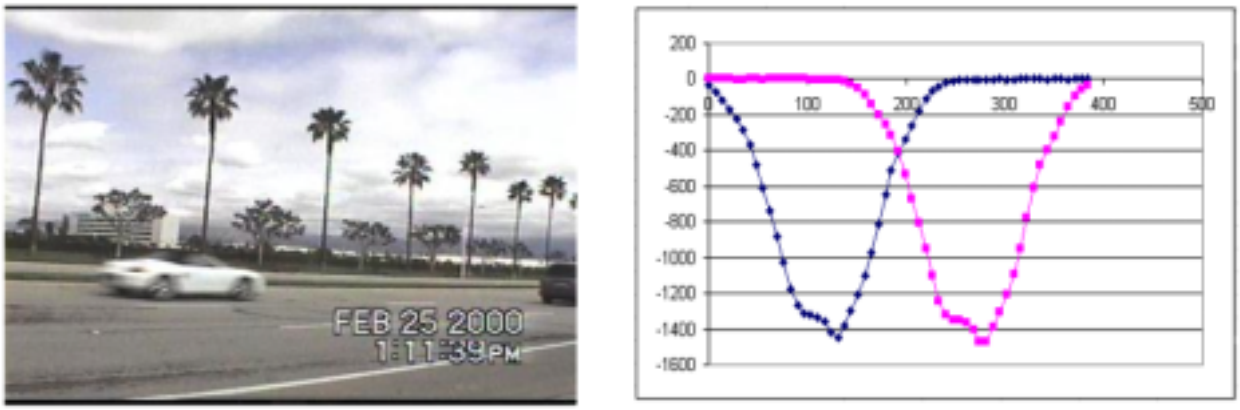


Figure 7 Passenger Car Signature

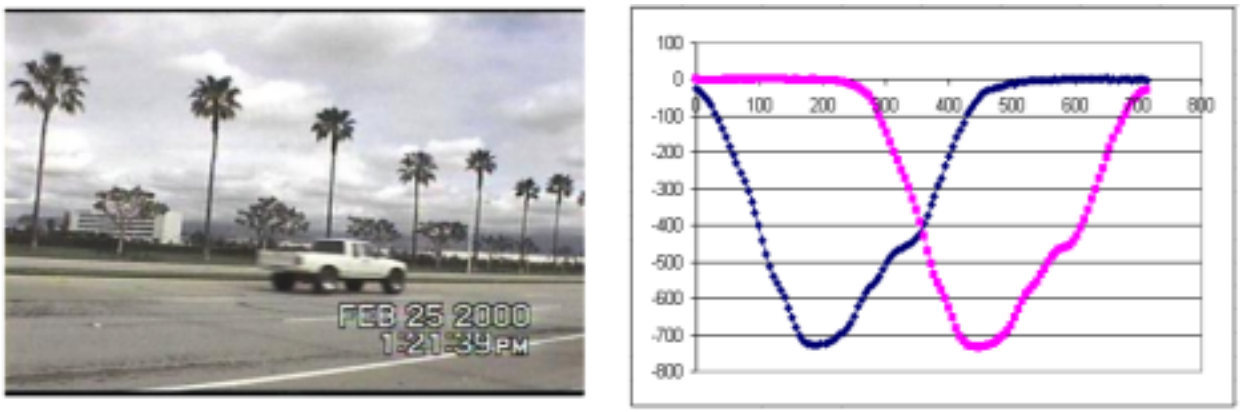


Figure 8 Pickup Truck Signature

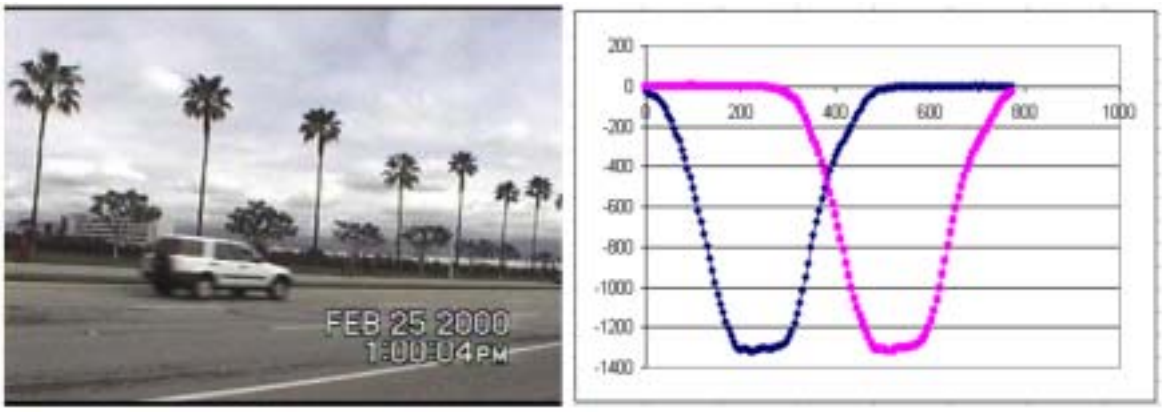


Figure 9 Sport Utility Car Signature

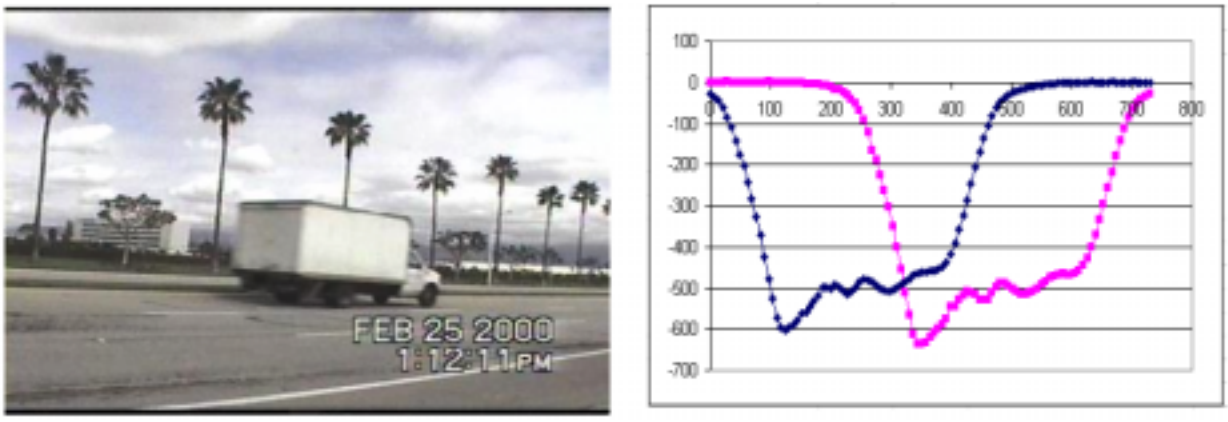


Figure 10 One Unit Truck Signature

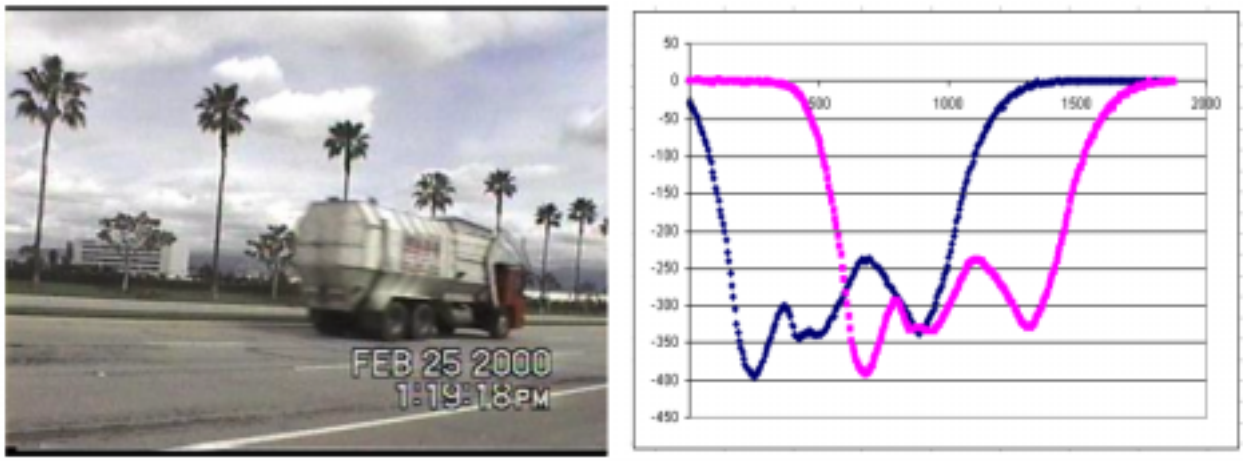


Figure 11 Trash Truck Signature

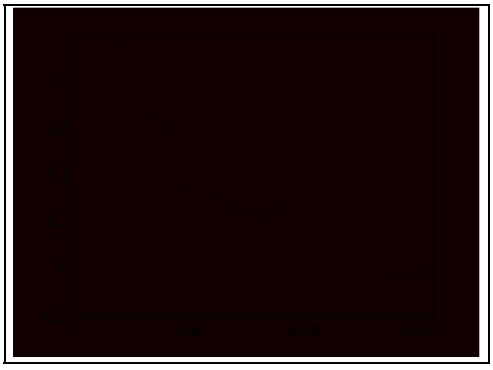


(a) Sample Vehicle Waveform

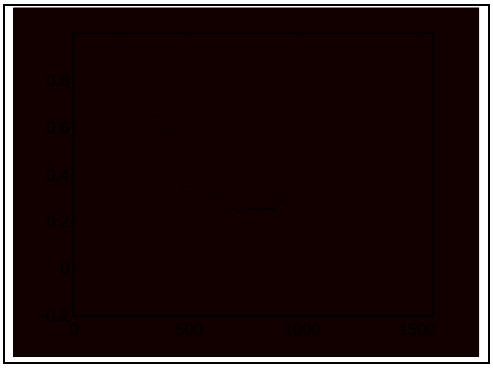


(b) Removal of Base Oscillations

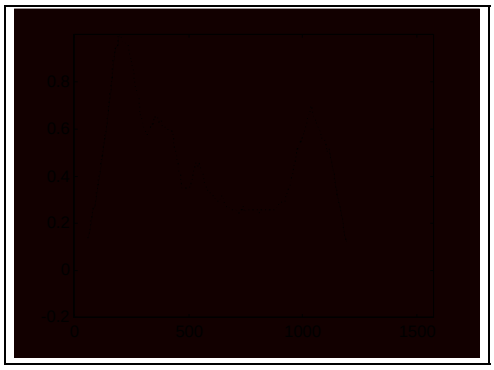


(c) Leading and Trailing Edge Slew Rates

Figure 12 Slew Rate Extraction Process

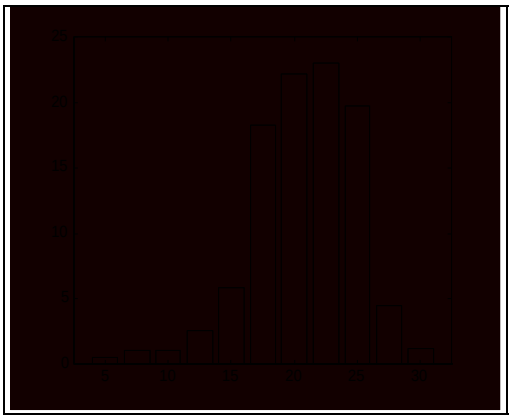

(a) AM Peak Downstream

(b) PM Upstream

Figure 13 Speed Distribution (Percent Relative Frequency)

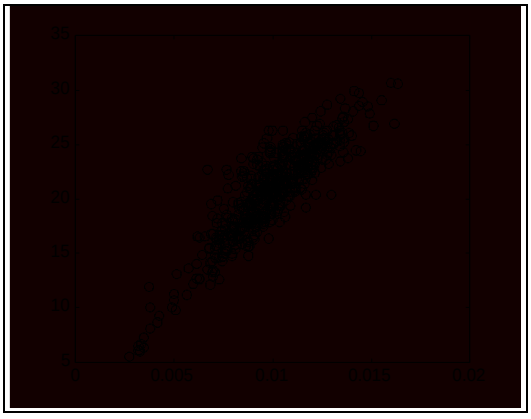

(a) AM Peak Downstream using Loop 1

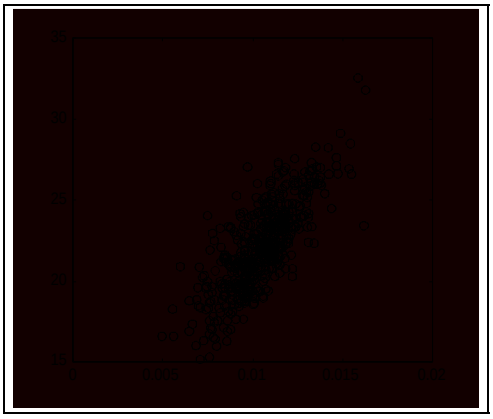

(b) PM Upstream using Loop 2

Figure 14 Scatter Plot of Slew Rate and Speed

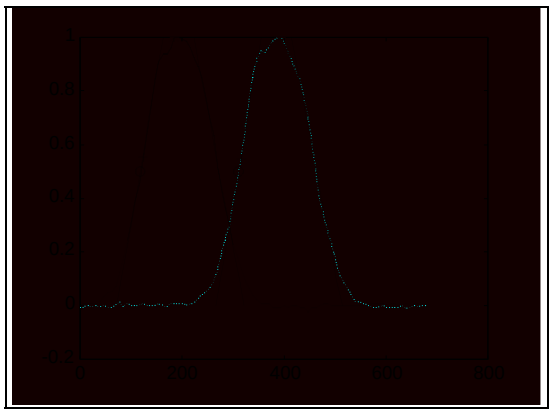


Figure 15 Double Loop Speed Computation using Waveforms

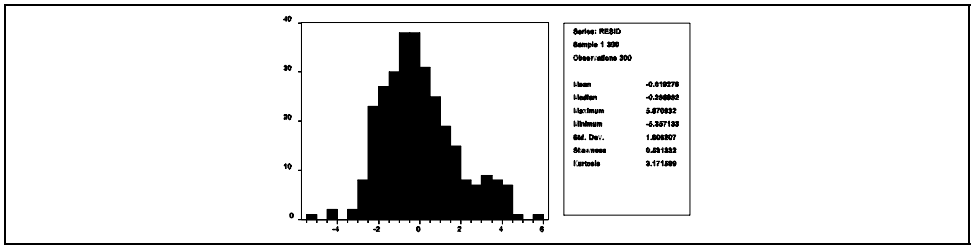


Figure 16 Regression Residual Analysis

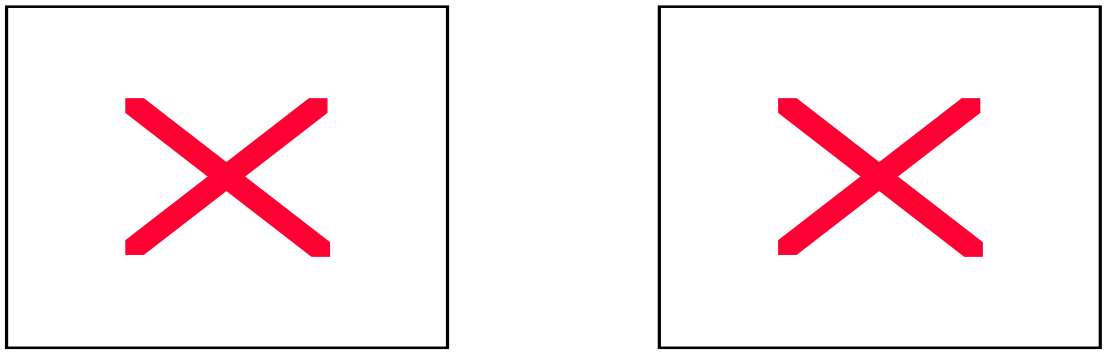

(a) Sensitivity of Regression Parameters (b) Sensitivity of Average Prediction Error

Figure 17 Sensitivity to Calibration Data Size

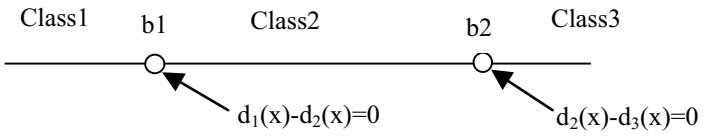


Figure 18 One-dimensional Pattern Recognition Example

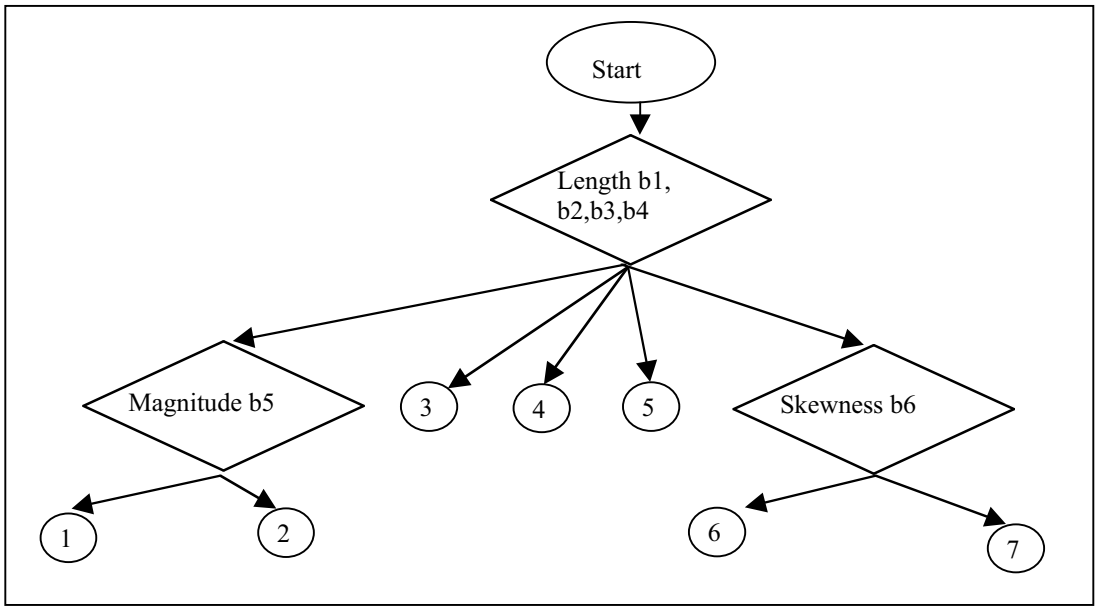


(a) Algorithm 1

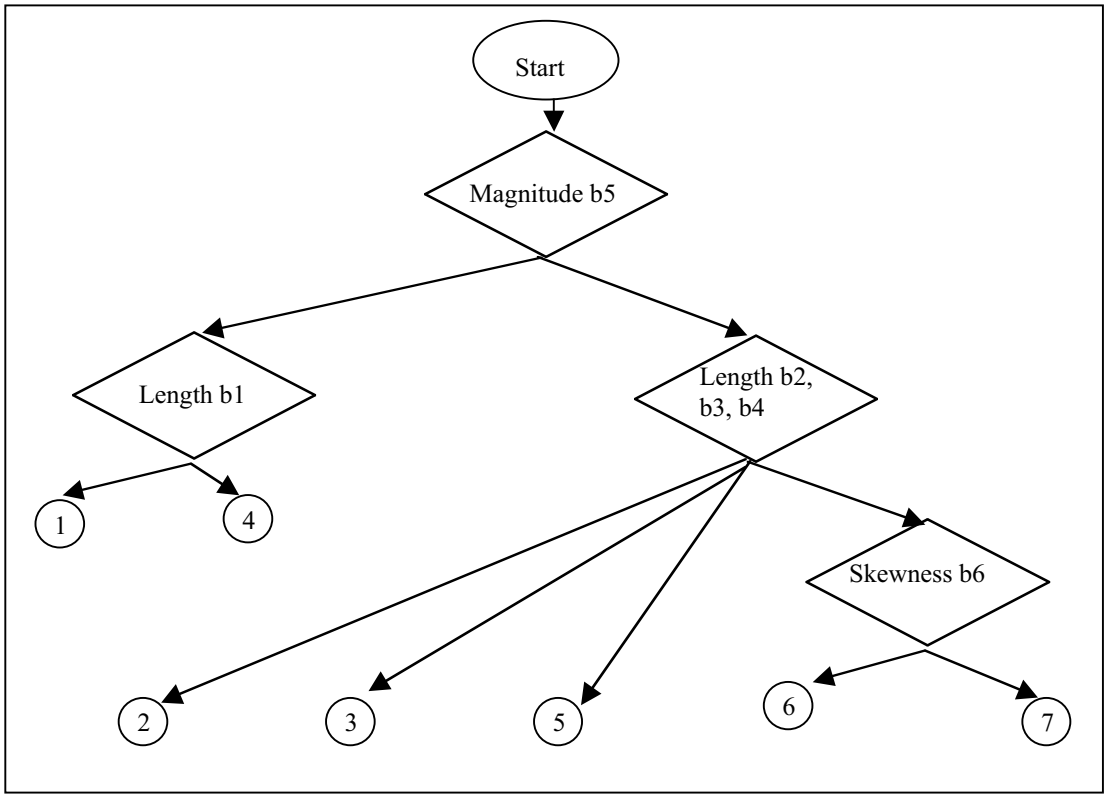


(b) Algorithm 2

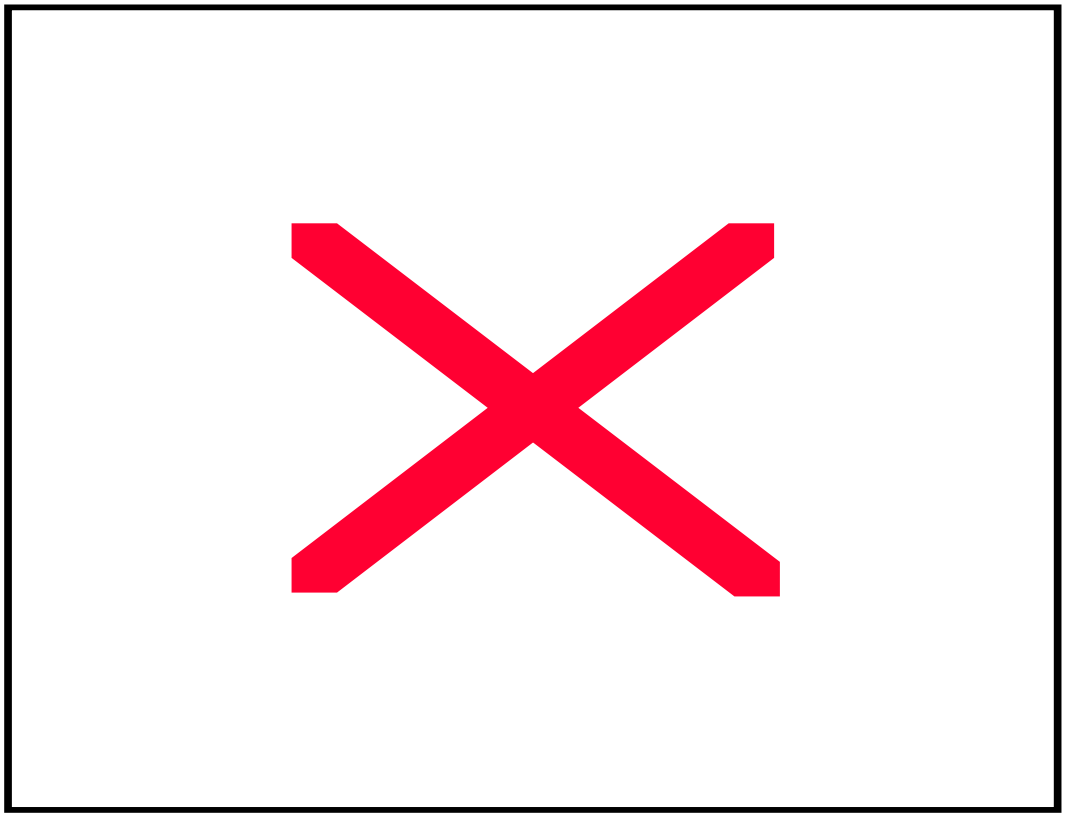

(c) Algorithm 3

Figure 19 Heuristic Algorithms

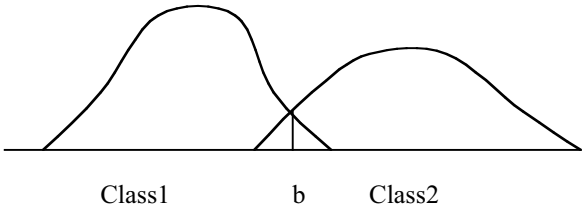


Figure 20 Example of Discrimination with Unimodal Feature Vector Distribution

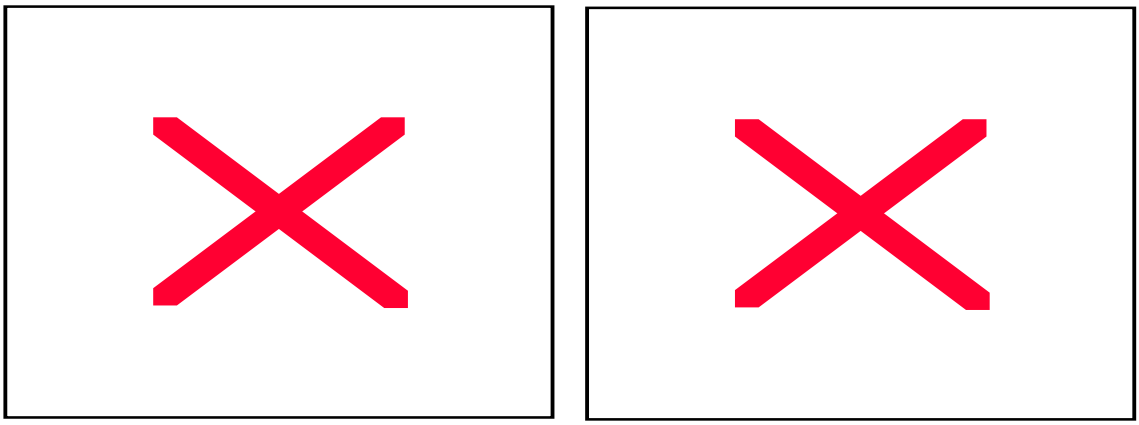

Figure 21 Examples of Unimodal Objective Functions using Vehicle Signature Length as Feature Vector

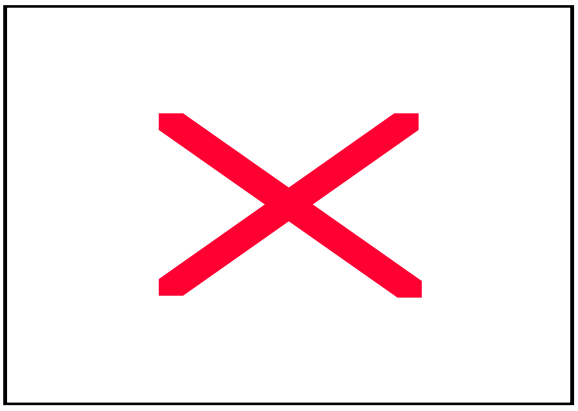

Figure 22 Incomplete Signature

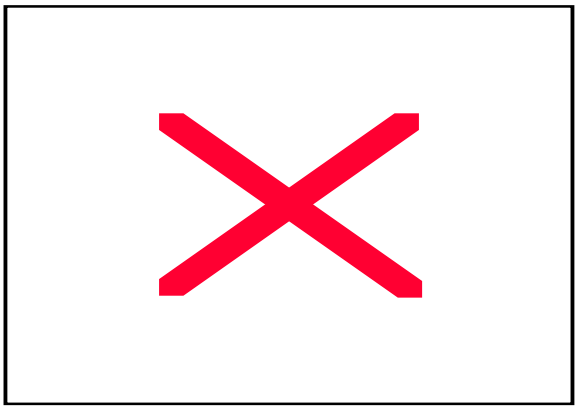

Figure 23 Partial Overlap Signature

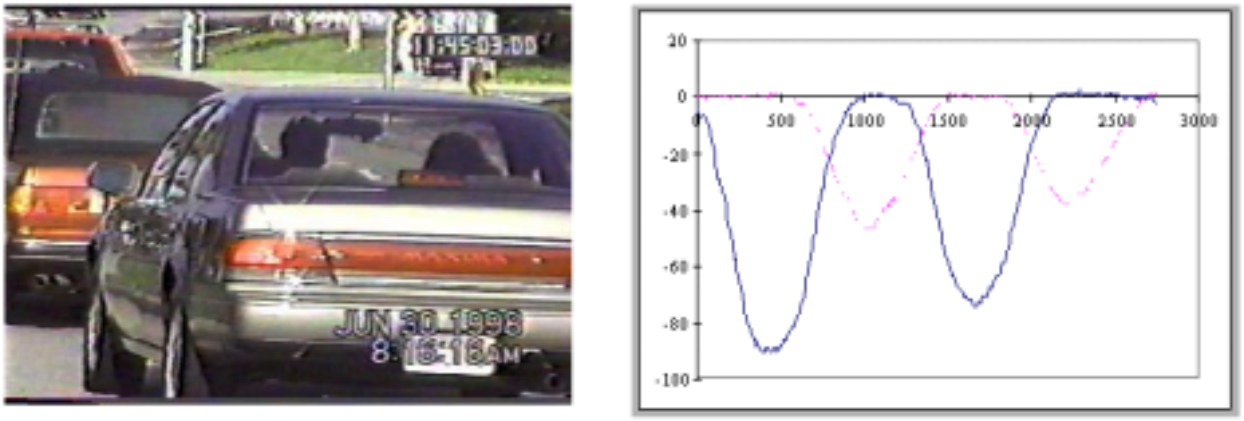


Figure 24 Tailgating Vehicles Signature

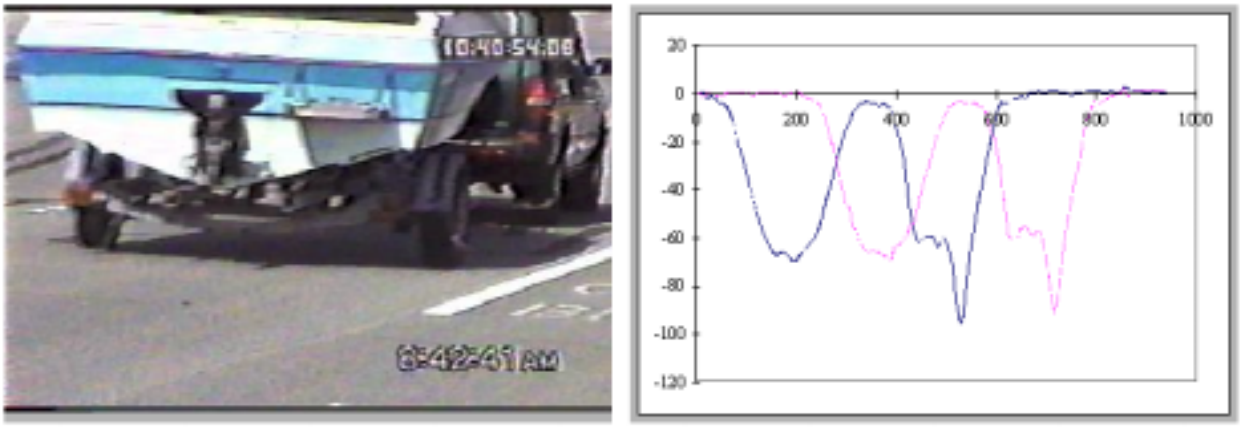


Figure 25 Vehicle with Boat Signature

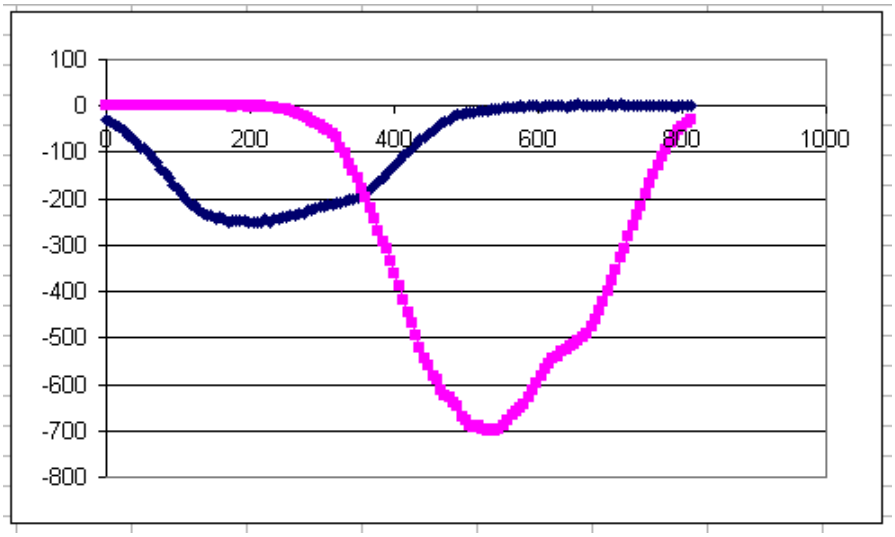


Figure 26 Turning Vehicle Signature (Pickup Truck)

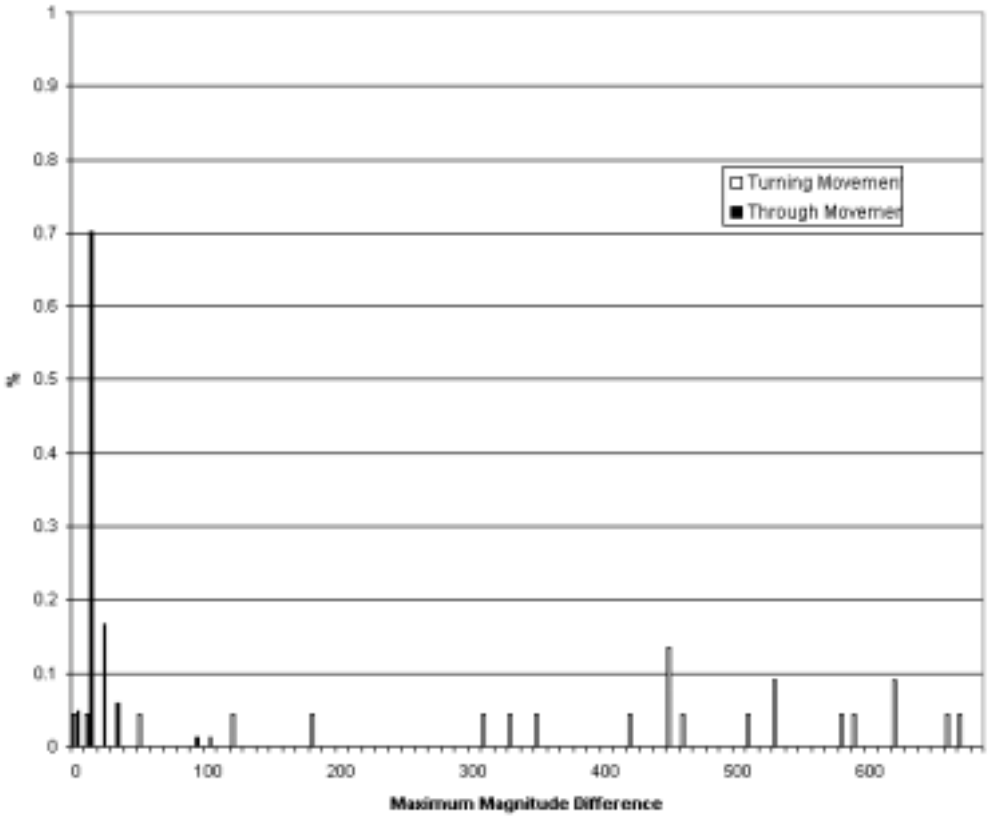


Figure 27 Maximum Magnitude Difference Distribution

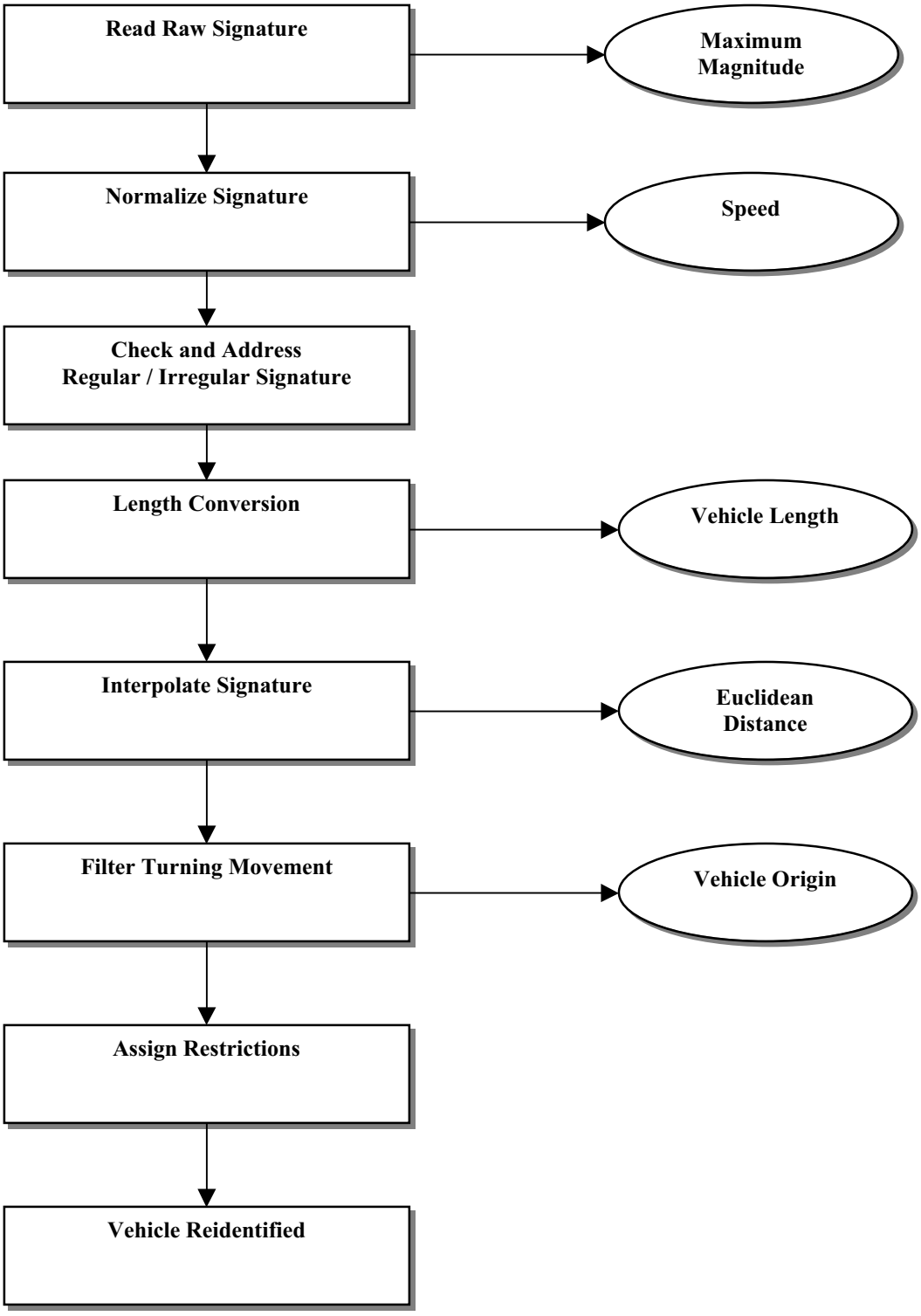


Figure 28 Modified Vehicle Reidentification Procedure

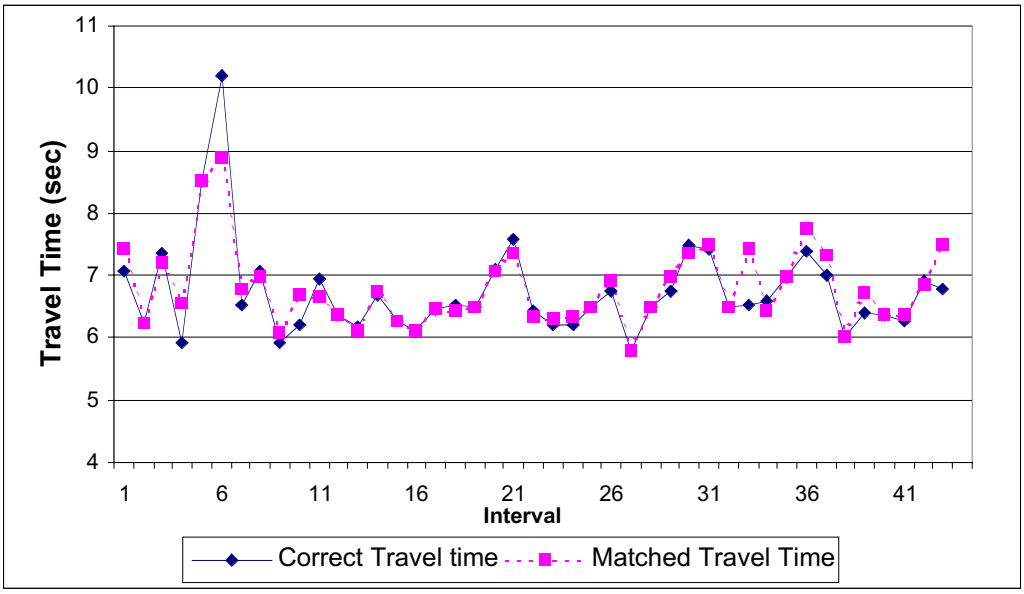


Figure 29 Average Section Travel Time

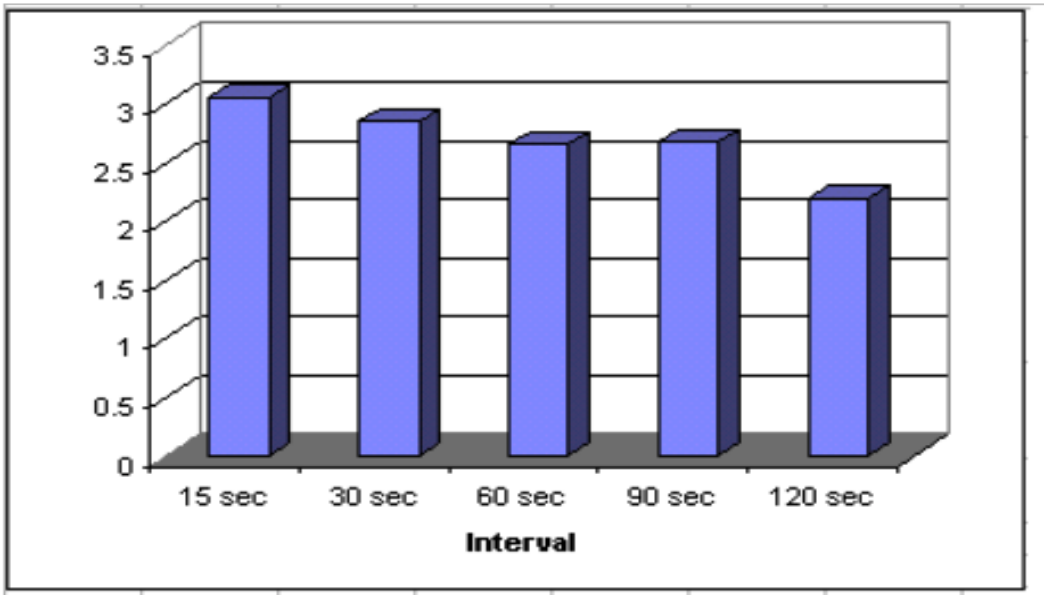


Figure 30 Travel Time Average Percentage Error

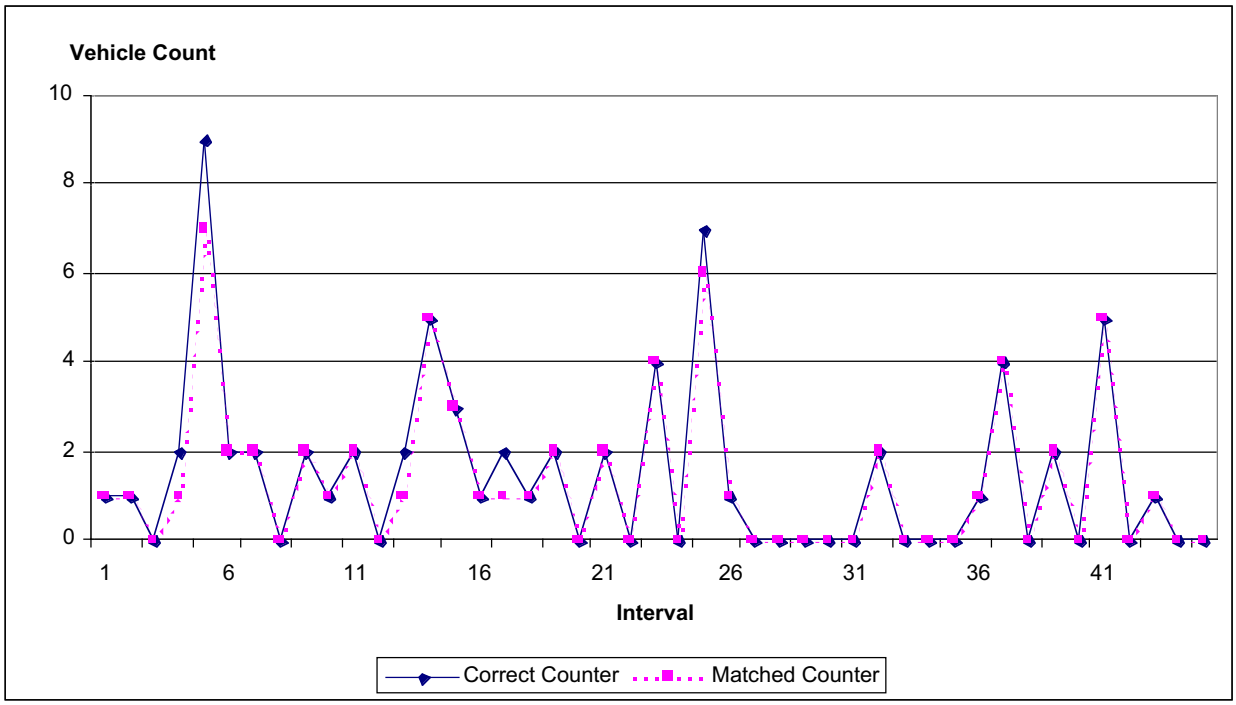


Figure 31 Average Section Density

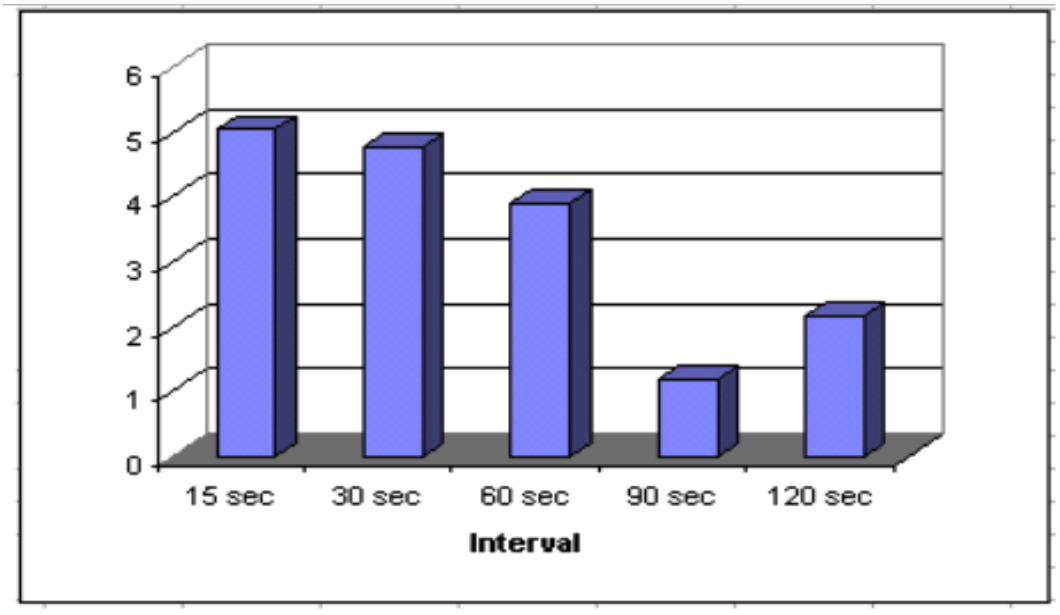


Figure 32 Density Average Percentage Error

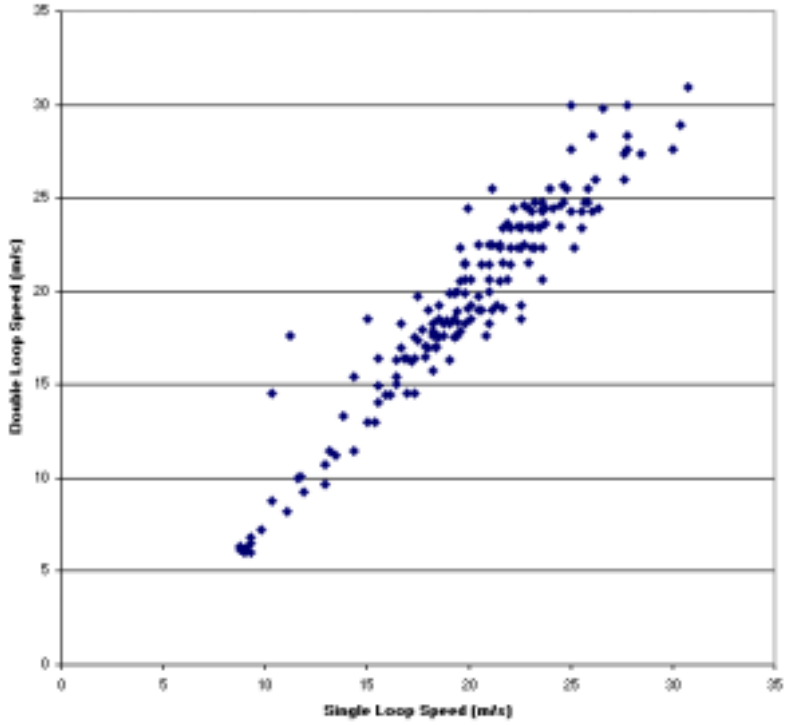


Figure 33 Double Loop Speed vs Single Loop Speed (Alton Parkway)

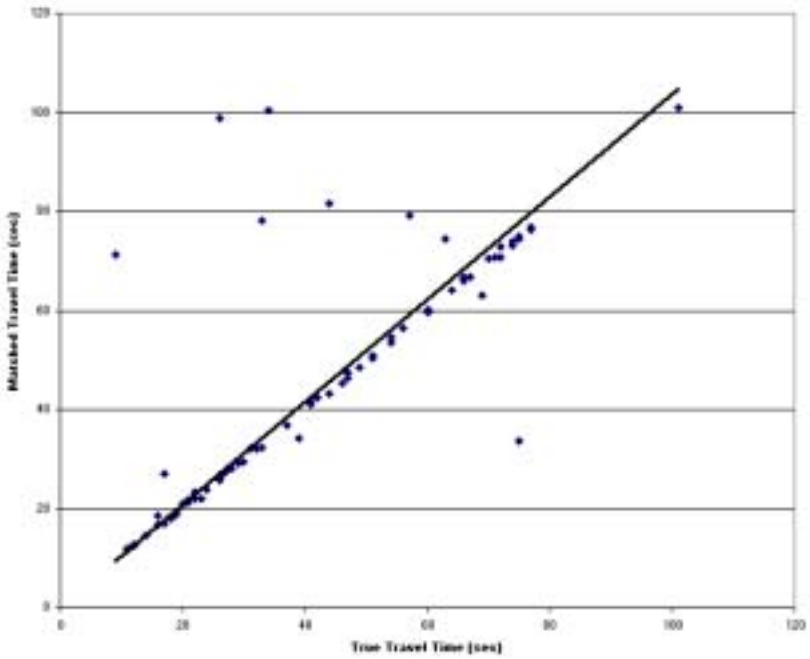


Figure 34 Travel Time Comparison : True Travel Time vs Algorithm Output Travel Time

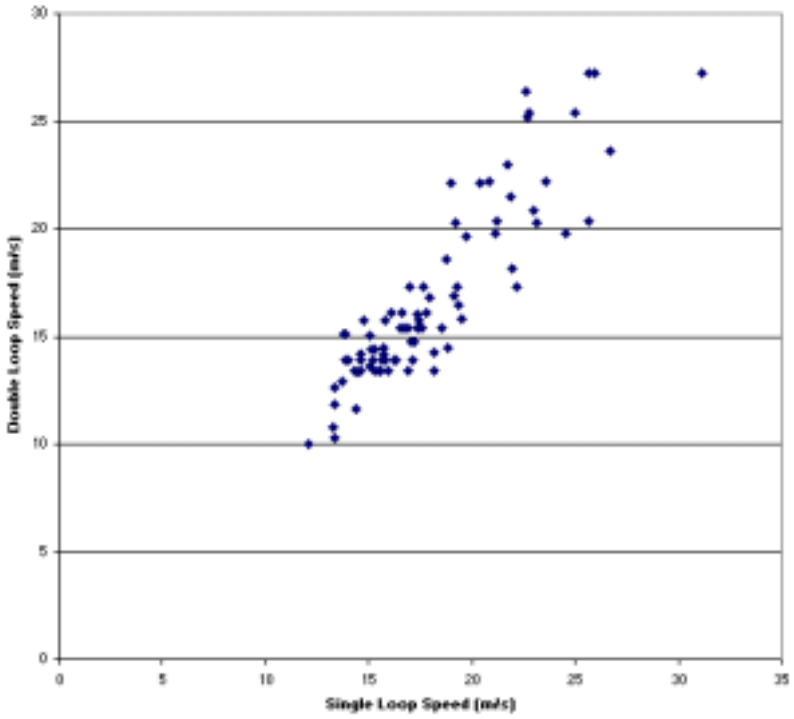


Figure 35 Double Loop Speed vs Single Loop Speed (Alton/ICD)

Table 1 Linear Regression Results

| Output<br>(1) | Coefficient<br>(2) | Standard Error<br>(3) | t-Statistic<br>(4) |
|---|---|---|---|
| a (intercept) | 3.597205 | 0.461335 | 7.797389 |
| b (slope) | 1739.639 | 46.04257 | 37.78327 |
| $R^2$ | 0.8273 | | |
| Standard Error of regression | 1.9028 m/s | | |

Table 2 Single Loop Speed Computation Results using AM Downstream Data

| Errors<br>(1) | Waveform Speed<br>(2) | Unbiased Speed<br>(3) | Biased Speed<br>(4) |
|---|---|---|---|
| Average Error (%) | 6.7 | 12.7 | 36.9 |
| Standard Deviation of Error (%) | 5.3 | 8.7 | 11.8 |

Table 3 Testing Transferability using AM Downstream Data

| Errors (1) | Waveform Speed Using Second Loop (calibrated) (1) | Waveform Speed Using First Loop (uncalibrated) (2) |
|---|---|---|
| Average Error (%) | 6.7 | 7.2 |
| Standard Deviation of Error (%) | 5.3 | 5.9 |

Table 4 Single Loop Speed Computation Results using PM Upstream Data

| Errors (1) | Waveform Speed (2) | Unbiased Speed (3) | Biased Speed (4) |
|---|---|---|---|
| Average Error (%) | 6.7 | 7.24 | 37.1 |
| Standard Deviation of Error (%) | 5.7 | 11.73 | 15.9 |

Table 5 Regression using Other Model Forms

| Output (1) | Coefficient (2) | Standard Error (3) | t-Statistic (4) |
|---|---|---|---|
| (a) Quadratic Model Form: speed = a + b slew + c slew$^2$ | | | |
| a | -1.838342 | 1.016288 | -1.808879 |
| b | 3028.725 | 221.9280 | 13.64733 |
| c | -70812.11 | 11953.21 | -5.924108 |
| $R^2$ | 0.845554 | | |
| Standard Error of regression | 1.802480 m/s | | |

Table 6 Seven Vehicle Class Scheme

| Class Code | 1 | 2 | 3 | 4 | 5 | 6 | 7 |
|---|---|---|---|---|---|---|---|
| Description | car, minivan, sports, station wagon | SUV, pickup | van, full-size pickup | limo | 2 axle truck | vehicle + trailer, bus | > 2 axle truck |

Table 7 Optimized Discriminant Bounds for Heuristic Algorithms

| Algorithm | b1 | b2 | b3 | b4 | b5 | b6 |
|---|---|---|---|---|---|---|
| Heuristic 1 | 15.94 | 19.97 | 26.37 | 33.01 | 1000 | 10 |
| Heuristic 2 | 16.87 | 16.77 | 21.68 | 29.67 | 1019.13 | 2.24 |
| Heuristic 3 | 21.729 | 983.172 | 15.910 | 1250.1 | 29.438 | 10 |

Table 8 Classification Results

| Algorithm/ Data | Overall Rate | Class 1 | Class 2 | Class 3 | Class 4 | Class 5 | Class 6 | Class 7 |
|---|---|---|---|---|---|---|---|---|
| Heuristic 1/Training | 84% | 86% | 92% | 81% | 100% | 50% | 100% | 75% |
| Heuristic 1/ Testing | 81% | 87% | 83% | 73% | 100% | 50% | 100 | 67% |
| Heuristic 2/ Training | 91% | 96% | 100% | 77% | 100% | 75% | 100% | 50% |
| Heuristic 2/ Testing | 82% | 87% | 96% | 69% | 67% | 75% | 50% | 50% |
| Heuristic 3/ Training | 88% | 93% | 88% | 77% | 67% | 88% | 100% | 75% |
| Heuristic 3/ Testing | 85% | 96% | 72% | 77% | 67% | 75% | 100% | 75% |

Table 9 Classification Results for Heuristic Algorithm 3

| | | Heuristic 3 Classification for Training Set | | | | | | |
|---|---|---|---|---|---|---|---|---|
| | | Class 1 | Class 2 | Class 3 | Class 4 | Class 5 | Class 6 | Class 7 |
| Correct Class | Class 1 | 64 | 4 | 1 | 0 | 0 | 0 | 0 |
| | Class 2 | 2 | 22 | 1 | 0 | 0 | 0 | 0 |
| | Class 3 | 4 | 2 | 20 | 0 | 0 | 0 | 0 |
| | Class 4 | 0 | 0 | 0 | 2 | 1 | 0 | 0 |
| | Class 5 | 0 | 0 | 1 | 0 | 7 | 0 | 0 |
| | Class 6 | 0 | 0 | 0 | 0 | 0 | 2 | 0 |
| | Class 7 | 0 | 0 | 0 | 0 | 1 | 0 | 3 |
| | | Heuristic 3 Classification for Test Set | | | | | | |
| | | Class 1 | Class 2 | Class 3 | Class 4 | Class 5 | Class 6 | Class 7 |
| Correct Class | Class 1 | 66 | 3 | 0 | 0 | 0 | 0 | 0 |
| | Class 2 | 1 | 18 | 6 | 0 | 0 | 0 | 0 |
| | Class 3 | 3 | 2 | 20 | 0 | 1 | 0 | 0 |
| | Class 4 | 0 | 0 | 0 | 2 | 1 | 0 | 0 |
| | Class 5 | 0 | 0 | 1 | 0 | 6 | 1 | 0 |
| | Class 6 | 0 | 0 | 0 | 0 | 0 | 2 | 0 |
| | Class 7 | 0 | 0 | 0 | 0 | 1 | 0 | 3 |

Table 10 Alton Parkway Reidentification Result

| DOWNSTREAM | | UPSTREAM | | | | | | Total |
|---|---|---|---|---|---|---|---|---|
| | | Passenger Car | Pickup Truck | SUV | Van | Truck/ Trailer | Bus | |
| Correctly Matched | | 328 | 43 | 66 | 35 | 3 | - | 475 |
| | Matching Rate (%) | 78.3 | 91.5 | 93.0 | 79.5 | 100 | - | 81.2 |
| Incorrectly Matched | Passenger Car | 29 | 1 | 1 | 4 | - | - | |
| | Pickup Truck | 1 | - | - | - | - | - | |
| | SUV | 8 | 2 | 2 | - | - | - | |
| | Van | 7 | - | - | - | - | - | |
| | Truck /Trailer | - | - | - | - | - | - | |
| | Bus | - | - | - | - | - | - | |
| | Subtotal | 45 | 3 | 3 | 4 | - | | 55 |
| Missed | | 46 | 1 | 2 | 5 | - | 1 | 55 |
| Total | | 419 | 47 | 71 | 44 | 3 | 1 | 585 |

Table 11 Alton Parkway Reidentification Result Comparison

| Vehicle Type | Number of Vehicles | Reidentification Result (Matching Rate %) | |
|---|---|---|---|
| | | Single Loop Speed | Double Loop Speed |
| Passenger Car | 101 | 66 (65.3) | 68 (67.3) |
| Pickup Truck | 26 | 20 (76.9) | 22 (84.6) |
| SUV | 35 | 29 (82.9) | 29 (82.9) |
| Van | 18 | 10 (55.6) | 12 (66.7) |
| Bus | - | - | - |
| Truck / Trailer | 2 | 2 (100) | 2 (100) |
| **Total** | **182** | **127 (69.8)** | **133 (73.1)** |

Table 12 Alton/ICD Data Description

| Upstream Lane 1 | | | Downstream Lane 1 | | | Matching |
|---|---|---|---|---|---|---|
| Through Vehicle | Different Lane at Downstream | 19 | Through Vehicle | Different Lane at Upstream | 6 | NA |
| | Matching at Downstream | 113 | | Matching at Upstream | 113 | 95 |
| Left Turning | | 8 | Left Turning | | 33 | NA |
| Right Turning | | 2 | Right Turning | | 0 | NA |
| Total | | 142 | Total | | 152 | |

Table 13 Alton/ICD Reidentification Result

| DOWNSTREAM | | UPSTREAM | | | | | | Total |
|---|---|---|---|---|---|---|---|---|
| | | Passenger Car | Pickup Truck | SUV | Van | Truck/ Trailer | Bus | |
| Correctly Matched | | 60 | 7 | 17 | 9 | 2 | - | 95 |
| | Matching Rate (%) | 80 | 100 | 85 | 100 | 100 | - | 84.07 |
| Incorrectly Matched | Passenger Car | 8 | - | - | - | - | - | |
| | Pickup Truck | - | - | 1 | - | - | - | |
| | SUV | 1 | - | 1 | - | - | - | |
| | Van | - | - | - | - | - | - | |
| | One Unit Truck /Trailer | - | - | - | - | - | - | |
| | Bus | - | - | - | - | - | - | |
| | Subtotal | 9 | - | 2 | - | - | - | 11 |
| Missed | | 6 | - | 1 | - | - | - | 7 |
| Total | | 75 | 7 | 20 | 9 | 2 | - | 113 |

Table 14 Alton/ICD Reidentification Result Comparison

| Vehicle Type | Number of Vehicles | Reidentification Result (Matching Rate %) | |
|---|---|---|---|
| | | Single Loop Speed | Double Loop Speed |
| Passenger Car | 75 | 51 (68) | 60 (80) |
| Pickup Truck | 7 | 6 (85.7) | 7 (100) |
| SUV | 20 | 14 (70) | 17 (85) |
| Van | 9 | 8 (88.9) | 9 (100) |
| Bus | - | - | - |
| Truck / Trailer | 2 | 2 (100) | 2 (100) |
| **Total** | **113** | **81 (71.7)** | **95 (84.1)** |